The PH domain as a mediator of Gβγ effector interactions

by

Osvaldo Cruz-Rodríguez

A dissertation submitted in partial fulfillment
of the requirements for the degree of
Doctor of Philosophy
(Chemical Biology)
in the University of Michigan
2017

Doctoral Committee:

Professor John J.G. Tesmer, Co-Chair
Professor Jorge A. Iñiguez-Lluhí, Co-Chair
Professor Anna K. Mapp
Professor Janet L. Smith
Professor John R. Traynor

Osvaldo Cruz Rodríguez

osvcruz@umich.edu

ORCID iD: 0000-0003-0801-8291

DEDICATION

To my father for inspiring me pursue my dreams, to my sister for teaching me the virtues of perseverance and to my wife, Gisselle, for all her love and continued support.

ACKNOWLEDGEMENTS

I am deeply indebted to past and present members of the Tesmer lab. Your willingness to share your knowledge and positivity enriched my experience as a graduate student immensely. Thank you deeply for your continued patience and support.

To John, I am particularly grateful for providing a space where creativity and exploration are encouraged.

Lastly, I'd like to acknowledge the generosity of Dr. Alan V. Smrcka and Dr. Heidi Ham. I will always remember my interactions with you and your respective groups fondly.

TABLE OF CONTENTS

LIST OF FIGURES

Figures

LIST OF TABLES

LIST OF ABBREVIATIONS

ATP – adenosine triphosphate

ATR-FTIR – attenuated total reflectance Fourier transform infrared

DAG – diacyl glycerol

CTD – C-terminal domain

CV – column volume

DNA – deoxyribonucleic acid

GDP – guanosine diphosphate

GPCR – G protein-coupled receptor

GST – glutathione S-transferase

GTP – guanosine triphosphate

GRK – G protein-coupled receptor kinase

HRP – horse radish peroxidase

HTH – helix-turn-helix

IP – inositol phosphate

IP3 – inositol 1,4,5-triphosphate

NTA – nitrilotriacetic acid

PBS – phosphate buffered saline

PE – phosphatidylethanolamine

PEI – polyethylenimine

PH – pleckstrin homology

PI – phosphatidylinositol

PIP – phosphatidylinositol phosphate

PIP2 – phosphatidylinositol 4,5- biphosphate

PIP3 – phosphatidylinositol 3,4,5- triphosphate

PKA – protein kinase A

PKD – protein kinase D

PKC – protein kinase C

PLC – phospholipase C

RH – regulator of G protein signaling homology

RNA – ribonucleic acid

ROCK1 – Rho-associated protein kinase 1

SFG – sum frequency generation

SUV – small unilamellar vesicle

TIM – triosephosphate isomerase

ABSTRACT

G protein βγ subunits regulate the activity, via direct interaction, of a large number of downstream effectors in GPCR signaling pathways. Whereas much is known about how these regulatory interactions impact cellular processes, less is understood about the structural determinants that mediate these interactions. Among the most extensively investigated Gβγ effectors are members of the PLCβ subfamily. PLC enzymes are a class of multi-domain phosphodiesterases that catalyze the hydrolysis of phosphatidylinositol 4,5-biphosphate to form two important second messengers, inositol 1,4,5-triphosphate and diacylglycerol. The activity of PLCβ isozymes is altered to varying extents by G protein α and βγ subunits as well as small GTPases. Several lines of biochemical and structural data have contributed to our understanding of the regulatory mechanisms that govern the activation PLCβ isozymes by $G\alpha_q$ subunits and Rac.

However, despite several reports suggesting that regions of the PH domain and the catalytic core contain critical residues for Gβγ binding, the manner by which Gβγ subunits stimulate the activity of PLCβ remains an unsolved problem. The work presented in this dissertation aims to examine the role of specific structural elements of the PH domain of PLCβ isozymes in mediating the response of this PLC subfamily to Gβγ. To that end, we used a combination of peptide array analysis, site directed mutagenesis and activity assays in both cell-based and reconstituted systems to map the structural determinants of the Gβγ interaction. Our results suggest that, although the

flexible loops along the PH/Rac1 interface, observed in the crystal structure of PLCβ2-Rac1 complex, do not participate in direct interactions with Gβγ they nonetheless contribute to activation. This work highlights the complexity of the Gβγ interaction and the importance of the PH domain towards activation of PLCβ by Gβγ.

GRK2, best known for its ability to phosphorylate active GPCRs, is another well -known Gβγ effector. Owing to its role in normal and diseased heart function there is great interest in the development of inhibitors of GRK2. Based on the structural analysis of two potent GRK2 inhibitors bound to the GRK2-Gβγ complex our lab previously proposed that the potency and selectivity of less potent GRK2 inhibitors, with improved pharmacological properties, could be enhanced using a structure-activity relationship guided design strategy. As part of this effort, I determined the co-crystal structure of the GRK2-Gβγ complex bound to a small molecule inhibitor of GRK2 based on a paroxetine scaffold. This novel inhibitor exhibited increased potency and selectivity towards GRK2 as well as improved contractility of cardiac myocytes relative to its parent compounds.

Additional work presented details my contribution to a study aimed at understanding the functional consequences of membrane lipid composition in relation to the orientation of the GRK2-Gβγ complex on lipid bilayers. This study revealed that the concerted binding of GRK2, via its PH domain, to Gβγ and PIP2 likely position the receptor docking site of GRK2 in orientation that optimizes its interaction with active GPCRs.

CHAPTER 1

INTRODUCTION

G protein-coupled receptor signaling

The ability of the cell to respond to external stimuli is central to its survival and proliferation. This inherent trait requires careful coordination of vast numbers of biological molecules in order to ensure that the appropriate elements of the cellular machinery are engaged. At the heart of this carefully orchestrated response is a class of membrane receptors known as G protein-coupled receptors. This family of membrane receptors represents the largest and most diverse group of signaling proteins with over 800 genes [1] that figure prominently in a large number of signaling pathways. Unsurprisingly, GPCRs have been the object of intense study for decades and this has led to the development of more than 20% of current drugs in the market [2]. Intriguingly, recent evidence for sustained endosomal signaling of select GPCRs through G protein independent pathways suggest a more nuanced role in signal transduction than originally ascribed to this class of membrane receptors [3,4].

All GPCRS are arranged in a seven transmembrane α-helical topology, an extracellular region comprised of the N terminus and three loops, and an intracellular region comprised of three intracellular loops, a short amphipathic helix and an extended C terminal tail. While these features are common among all GPCRs, members of this superfamily of proteins are associated with widely divergent cellular processes and their

classification into eleven subfamilies has been primarily based on the types of inputs they respond to [1,5]. As their namesake suggest, GPCRs are intimately associated with a class of guanine nucleotide-binding heterotrimeric proteins commonly referred to as G proteins. Functionally, the G protein heterotrimer is made up of two distinct functional components, Gα and Gβγ, and both signaling proteins are able to regulate the activity of a wide range of effectors (Fig. 1.1). The inherent capacity of a GPCR to engage specific pools of either G protein subunit directly influences the type of cellular response elicited by their activation [6].

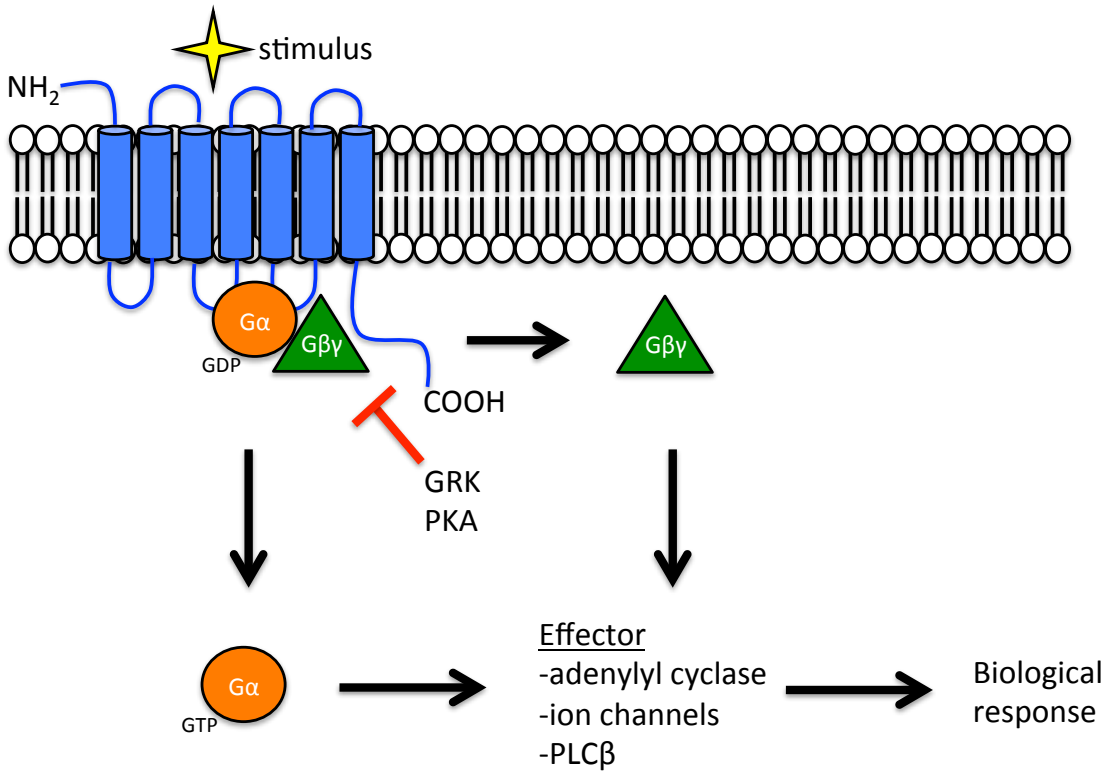

Figure 1.1. Overview of GPCR signaling. Stimulation of a GPCR by external stimuli results in receptor catalyzed exchange of GDP for GTP and concomitant dissociation of the G protein heterotrimer. A given biological response is the result of the coordinated interactions of both Gα-GTP and Gβγ subunits with a wide array of cellular effectors.

Similar to the diversity observed among GPCRs, the number of signals that can initiate a GPCR mediated response is staggering and range from small organic molecules, such as

epinephrine and morphine, to peptides, lipids and even a single photon of light. Regardless of the type of input signal, activation of a GPCR leads to a conformational change in the receptor that promotes the exchange of GDP for GTP in the Gα subunit. This receptor catalyzed nucleotide exchange on the Gα subunit leads to the dissociation of the heterotrimer. Whereas early studies suggested a more prominent role for the Gα subunit in G protein mediated signaling, more recent evidence highlights an increasingly expansive role for Gβγ in mediating the cellular response to external stimuli [7–9].

Structure and function of Gβγ

Despite its heterodimeric nature, the Gβγ complex functions as a unit and its dissociation can only achieved through the use of denaturants [6]. Several isoforms of both β ($G\beta_{1\text{-}5}$) and γ ($G\gamma_{1\text{-}5,7\text{-}13}$) subunits exist, however, their functional roles, subunit specificity and abundance are not as clearly defined as is the case with the Gα subunit[7,9]. In additional contrast to the Gα subunit, the expression of Gβγ requires several eukaryotic chaperone complexes required for proper folding of both Gβ and Gγ as well as assembly of the dimer, limiting its expression to eukaryotic hosts [8]. Atomic structures of Gβγ have revealed that the γ-subunit has a simple extended α-helical fold that associates with the α helical N-terminal region of Gβ via formation of a coiled coil and then wraps around one side of the Gβ barrel. The N-terminal region of the Gβ subunit is followed by a β-propeller assembly of seven WD repeats, with each of the blades of the propeller being formed by four anti-parallel β strands (Fig. 1.2A)[10].

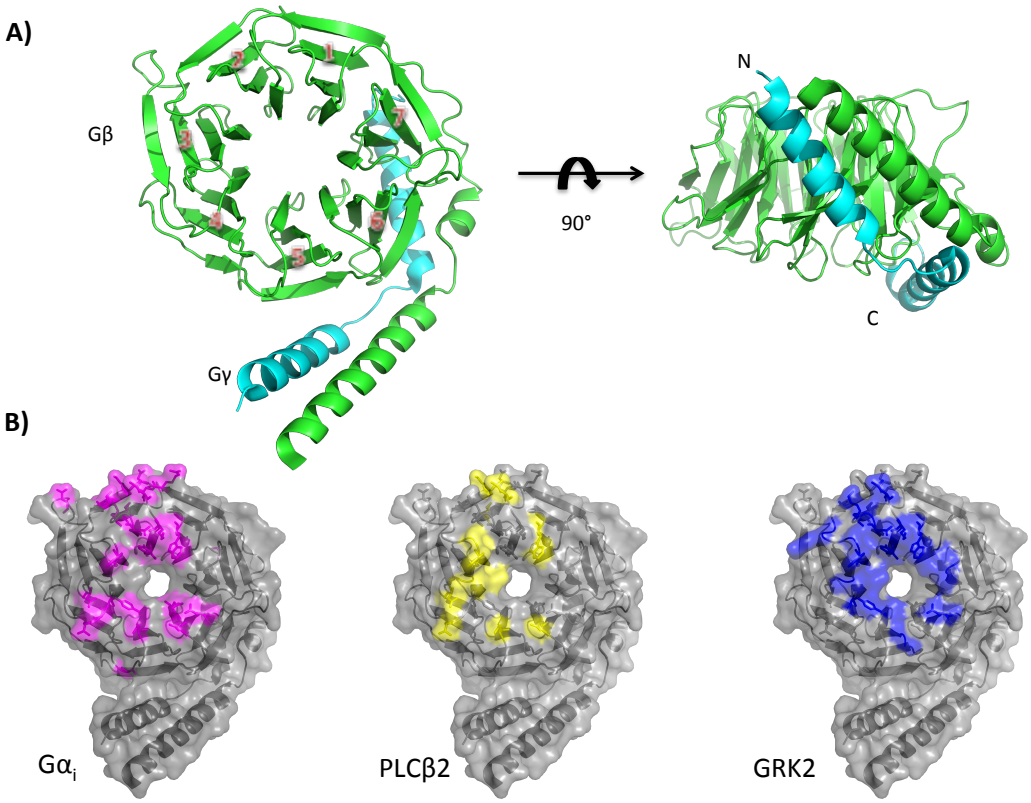

Figure. 1.2. General structure and effector-binding surface of G protein βγ subunits. A) The β subunit fold is typical of other WD repeat proteins and consists of a β propeller assembly of seven blades. Four anti-parallel β sheets form each blade of the propeller. The γ-subunit (cyan) forms contacts with both the N-terminal α-helical segment and blades 6 and 7 of the β subunit. B) Surface representation of Gβγ effector binding interfaces for Gα$_i$, PLCβ2 and GRK2. While effector interactions occur along the same surface of Gβγ, each effector contacts a different subset of the residues that make up this surface. The regions of this surface in contact with Gα$_i$, PLCβ2 and GRK2 are shown in magenta, yellow and blue respectively.

The Gβγ complex associates with the cell membrane via a prenyl moiety attached to the C terminus of the γ-subunit. The nature of the isoprenoid group, either farnesyl or geranylgeranyl, is dependent on the specific residues contained within a conserved C-terminal sequence, generally denoted as the CAAX motif, consisting of a cysteine residue which precedes two aliphatic residues followed by an amino acid of variable identity [11]. Additional elements upstream of this motif have been implicated in determining the specific lipid moiety attached [12].

The contribution of prenylation of the γ subunit to effector binding seemingly varies from effector to effector. For instance, type II adenylyl cyclase is activated exclusively by Gβγ dimers containing a geranylgeranyl group. In contrast, PLCβ isoforms are activated by Gβγ dimers modified with either prenyl group, albeit with different potencies [13].

Gβγ has several canonical effectors, such as Kir3 channels, voltage dependent Ca^{2+} channels, several phospholipase C and adenylyl cyclase isoforms, PI3K and MAPK [7,8,10]. Notably, these effectors interact with Gβγ through an interface that overlaps with the Gα interaction surface (Fig. 1.2B), leading several investigators to propose targeting this interface with peptides and small molecules as a means of selectively disrupting Gβγ mediated activity [14–17]. Although development of small molecule inhibitors of Gβγ has led to several promising leads, these efforts have been limited by the lack of structural data on Gβγ small molecule complexes.

More recently, several non-canonical Gβγ effectors, such as histone deacetylase 5, the glucocorticoid receptor, protein kinase D and soluble N-ethylmaleimide-sensitive factor activating protein receptor (SNARE) proteins have been described [9]. Notably, these non-canonical Gβγ-effector interactions seem to occur at several different subcellular compartments. Evidently, a generalized mechanism for Gβγ mediated functions of both novel and canonical effectors does not exist. However, studies of Gβγ dependent activity of different canonical effectors have revealed two potential recurring mechanisms: membrane recruitment and Gβγ induced conformational changes. The dissertation presented here is an examination of the mechanisms that govern the regulation of two canonical effectors, PLCβ and GRK2, by Gβγ.

Phospholipase Cβ isozymes and their regulation by Gβγ

PLC isozymes are perhaps best known for their ability to catalyze the hydrolysis of the inner leaflet phospholipid PIP2 [18]. This simple reaction has some rather far-reaching consequences. First, both reaction products, IP3 and DAG, function as important second messengers capable of inducing mobilization of intracellular Ca^{2+} stores and activation of PKC. Additionally, because PIP2 is a precursor for PIP3, the catalytic activity of PLC is intrinsically linked to numerous phosphoinositide-dependent signaling pathways and the phosphoinositide binding proteins whose functions depend on the relative abundance of either phosphoinositide [19]. To date, thirteen different mammalian PLC isozymes have been identified and subsequently organized into six families on the basis of sequence similarity [20].

PLCβ isozymes (PLCβ1-4) and their regulation by heterotrimeric G proteins have been the subject of intense investigation [21–23]. Like other members of the PLC superfamily, PLCβ isozymes are multi-domain proteins in which several modular domains flank a split TIM barrel containing the active site (Fig. 1.3A). The three-dimensional structure of the catalytic core resembles a triose phosphate isomerase barrel domain. In PLCβ, the core is split into X and Y halves and is immediately preceded by a pleckstrin homology domain and 4 EF hand motifs (Fig. 1.3B). The X and Y halves are linked by a stretch of approximately 100 amino acids generally referred to as the X-Y linker. A C2 domain and a ~400 amino acid C terminal domain, the distinguishing feature of PLCβ isozymes, follow the catalytic core [24].

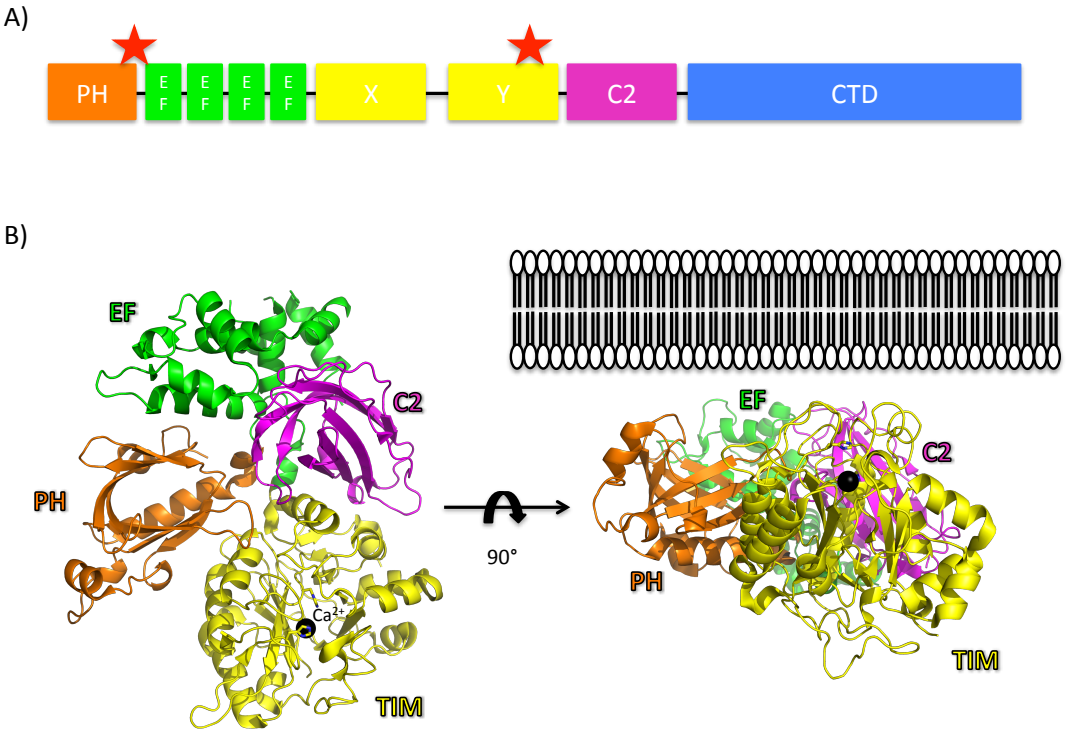

Figure 1.3 Phospholipase Cβ domain organization and structure. A) PLCβ isozymes consist of an N-terminal pleckstrin homology domain, four EF hand motifs, a split TIM barrel, C2 domain and C-terminal region. The active site residues are contained within the TIM barrel. Red stars indicate regions of PLCβ previously implicated in Gβγ mediated activation. B) Three-dimensional structure of PLCβ2 showing the spatial relationships among its domains [25]. The perspective depicted here represents an approximate orientation of PLCβ relative to the membrane.

The activity of PLCβ is subject to auto-inhibition by the X-Y linker. This seems evident from the existing PLCβ structures where C-terminal regions of the X-Y linker are observed to directly occlude the active site. Perhaps more convincing is the observation that disruption or deletion of the X-Y linker result in increased basal activity towards both membrane bound PIP2 and a soluble fluorescent analog [26,27]. The study of $G\alpha_q$ mediated activation of PLCβ and the elucidation of its underlying mechanism has led to the recognition of an additional auto-inhibitory element within PLCβ [28,29]. The mechanism involves extraction, by $G\alpha_q$, of a short

helix-turn-helix motif that otherwise binds tightly to the catalytic core and lies in close proximity to both active site and X-Y linker. Based on the observation that disruption of the interactions between the HTH and the catalytic core result in decreased thermal stability and increased basal activity, Lyon et al. proposed that binding of the HTH motif to the catalytic core contributes to the persistence of an auto-inhibited state by stabilizing the interactions of the X-Y linker with the enzyme.

In sharp contrast to our understanding of how PLCβ activity is regulated by $G\alpha_{q,}$ the manner by which Gβγ promotes increased activity of PLCβ remains uncertain. Of the four known isoforms of PLCβ, only PLCβ2 and PLCβ3 show an appreciable response to Gβγ [20,24]. Conspicuously, data supporting a discrete Gβγ binding site on PLCβ is conflicting. Evidence supporting two different regions of PLCβ, the PH domain and the catalytic core, exist. Whether these two regions are mutually exclusive as a de facto binding site remains to be seen but what is evident is that both can play a role in Gβγ mediated activation.

Early evidence supporting a critical role for the catalytic core in Gβγ mediated activation of PLCβ was based on studies using fragments derived from the Y region of the catalytic core to inhibit Gβγ mediated activation of full length PLCβ2 in transiently transfected cells [30]. Subsequent crosslinking studies employed peptides derived from the initially identified region of PLCβ2 to further delineate the region of interest to residues to 574-583 [31]. Of particular interest is the observation that triple alanine substitution of residues 574-576 in PLCβ2 impaired binding to Gβγ [32].

The PH domain as a potential Gβγ binding site is rather interesting proposition since several distantly-related PH domains have been shown to bind Gβγ [33]. This trend seemingly extends to other PLC isozymes because the isolated PH domains of PLCβ1-3 and PLCδ1 have

both been shown to bind to Gβγ [34,35]. Evidently, there is a poor correlation between the properties of these isolated domains and the corresponding native enzymes as only PLCβ2 and PLCβ3 have been shown to be responsive to stimulation by Gβγ. A more convincing argument in support of PH domain was made by Wang et al [36] using a chimeric construct where the PH domains of PLCδ1 and PLCβ2 were swapped in a backbone of PLCδ1. The responsiveness of the resulting chimera to Gβγ was comparable to PLCβ2 demonstrating a crucial role for the PH domain of PLCβ2 in conferring sensitivity to Gβγ.

More recently, Kadamur et al [35] identified a region of the PH domain of PLCβ3 purported to be involved in direct binding to Gβγ on the basis of homology to the PH domain of GRK2. Using interdomain crosslinking of the native enzyme and competition binding experiments the authors argue that this Gβγ binding site, which is buried in the PH/EF interface observed in the crystal structures of both PLCβ2 and PLCβ3, is exposed upon intrinsic movements of the PH domain. Han et al [37] has proposed similar two state models although in this case the available crystal structures of PLCβ are suggested to represent an active state and the Gβγ binding site lies on the opposite side of the PH domain. Clearly, a structure of a Gβγ-PLCβ complex would settle the debate over the mechanism that leads to Gβγ mediated activation of PLCβ. Until then, a deeper understanding of the role of PH domain might provide further insights into the regulation of PLCβ by Gβγ.

GRK2 subfamily and its interaction with Gβγ

Perhaps the best-known examples of a membrane translocation dependent Gβγ effector are two members of the GRK family of kinases, GRK2 and GRK3 [38,39]. The primary function ascribed to this class of enzymes is the phosphorylation of activated GPCRs, a critical step in the

desensitization of GPCR mediated signaling. Several reports suggest that the physiological functions of GRK2/3 extend beyond its conventional role in the internalization and trafficking of GPCRs [40]. Indeed, the activity or deregulation of GRK2/3 activity has been associated with cardiac [41] and inflammatory [42] disease as well as cancer [43]. Notably, despite a high sequence identity (>80%), distinct roles for both GRK2 and GRK3 have been reported for several disease states [44,45].

The structure of a GRK2 subfamily member consists of a regulator of G protein signaling homology domain that is interrupted by the highly conserved catalytic domain, a common structural feature among GRKs [46]. The overall structure of the catalytic core is consistent with that of other AGC kinases in which the active site is harbored in the junction between small and large lobes. A C-terminal region, generally referred to as the C-tail, extends over the active site. The region of the C-tail that lies directly above the active site, termed the active site tether, is generally the most disordered region in structures of inactive AGC kinase domains [47–49]. Upon binding, the adenine ring of ATP forms several contacts with the hinge joining the small and large lobes. In addition to these hinge contacts, kinase inhibitors occupy several subsites whose naming has been based on the respective structural subsites occupied by ATP [47].

The role of GRK2 in heart failure has garnered widespread interest in the development of selective inhibitors. Over the years, several different compounds, including, polyions, RNA aptamers, and peptides, have been evaluated as potential inhibitors of GRK2 [50]. More recently, several heterocyclic compounds whose structure mimic that of ATP have successfully been used as scaffolds in the development of GRK2 inhibitors with enhanced selectivity [51]. Notably, the application of small molecule inhibitors in structural studies of members of the GRK4 subfamily has led to further insights into the conformational dynamics of this class of enzyme [52,53].

Unlike other members of the GRK family, which are anchored to the membrane by lipid modifications of their C terminus, the carboxyl terminal region of GRK2/3 harbors a Gβγ-binding PH domain. Comparison of the crystal structures of GRK2 and a GRK2-Gβγ complex reveal that GRK2 does not undergo a significant conformational change upon binding to Gβγ [54]. This suggests that the role of Gβγ in mediating the activity of GRK2/3 is solely to recruit it to the membrane. However, the observation that Gβγ binding alters the orientation of GRK2 relative to the membrane in a manner that would promote of GRK2-GPCR interactions hints at a more complex mechanism [55].

The recurrence of the PH domain among several Gβγ effectors, such as a GRK2 and PLCβ, and the affinity of several isolated PH domains towards Gβγ in vitro has led to its implication as a Gβγ interaction motif [56]. While it might be tempting to ascribe a generalized function to the PH domain, its role in mediating Gβγ induced activation of effectors is seemingly more complex as illustrated by the distinct functional roles of the PH domains of GRK2 and PLCβ. Notably, how such interactions are influenced by their proximity to the cell membrane remains unclear. Herein we employ a combination of mutagenesis, functional assays and structural analysis to illustrate how, despite their structural similarities and affinity for Gβγ, the PH domains of two canonical effectors contribute differentially to Gβγ mediated activation. Our results highlight the importance of the plasma membrane in mediating the interactions between Gβγ and its effectors at the cytosol-membrane interface.

CHAPTER 2

THE ROLE OF SOLVENT EXPOSED REGIONS OF THE PH DOMAIN IN Gβγ MEDIATED ACTIVATION OF PLCβ

Introduction

PLC enzymes are a class of modular proteins that catalyze the hydrolysis of PIP2 into two important signaling molecules, DAG and IP3. Because this reaction is associated with a wide array of signaling pathways and cellular processes, the activity of PLC is tightly regulated [18,20,57]. In mammals, several PLC enzymes have been identified and among these, the PLCβ subfamily (PLCβ1-4) and their regulation by G proteins have been studied extensively [24]. Indeed, our current understanding of the underlying mechanistic details associated with a subset of the regulatory inputs to which PLCβ is subject is increasingly supported by several lines of evidence. The manner in which Gβγ promotes enhanced activity of PLCβ, however, remains an elusive and important piece of the puzzle.

The response of PLCβ to stimulation by Gβγ differs among the four known isozymes: PLCβ2>PLCβ3>PLCβ1 whereas PLCβ4 is non-responsive. Previous reports have implicated the PH domain and regions of the Y half of the TIM barrel in the activation of Gβγ sensitive isoforms [7,20,24,58]. A chimeric protein in which the PH domain of PLCδ1 was substituted for the corresponding domain of PLCβ2 has provided the most

compelling argument for a critical role for the PLCβ PH domain in mediating Gβγ responsiveness. Unlike its native counterpart, this PLCβ2/PLCδ1 chimera could be stimulated by Gβγ with comparable potency to PLCβ2, suggesting that the PH domain harbors sufficient structural determinants for conferring Gβγ sensitivity of PLCβ [36].

Although well known for their affinity for membrane surfaces and phosphoinositides, PH domains are recognized for their role in mediating protein-protein interactions in a large number of signaling proteins [59,60] and several different PH domains, including those of PLCβ, have been shown to bind to Gβγ directly. Whether this interaction translates to intact PLCβ is uncertain in part because the surface that is used to bind Gβγ in GRK2 is sequestered in PLCβ. Moreover, the specific role of the PH domain in promoting increased activity of select PLCβ isozymes in response to Gβγ is limited by our lack of understanding of the structural determinants that define its interaction with both Gβγ and the other domains of PLCβ.

The existing crystal structures of both holoenzyme and effector bound PLCβ reveal that the PH domain makes extensive contacts with the X half of the TIM barrel and the EF hand motifs. As the relative position of domains that form PLCβ is the same in all these structures it has been presumed that PLCβ isozymes do not undergo any large conformational change upon effector binding. If indeed this is the case the exposed surfaces of the PH domain most likely to interact with Gβγ would be limited to the PH/ Rac1 interface seen in the structure of the PLCβ2-Rac1 complex [25] and the cleft formed by the PH domain and the X domain of the TIM barrel.

Herein, we examine the role of several solvent exposed loops of the PH domain and the adjoining EF hand motif (Fig. 2.1A) and assess their contributions to both direct binding and activation of PLCβ by Gβγ. Our results provide additional structural insights into the regulation

of PLCβ isozymes and raise a number of intriguing questions regarding the functional role of the PH domain in modulating the activity of this canonical Gβγ effector.

A)

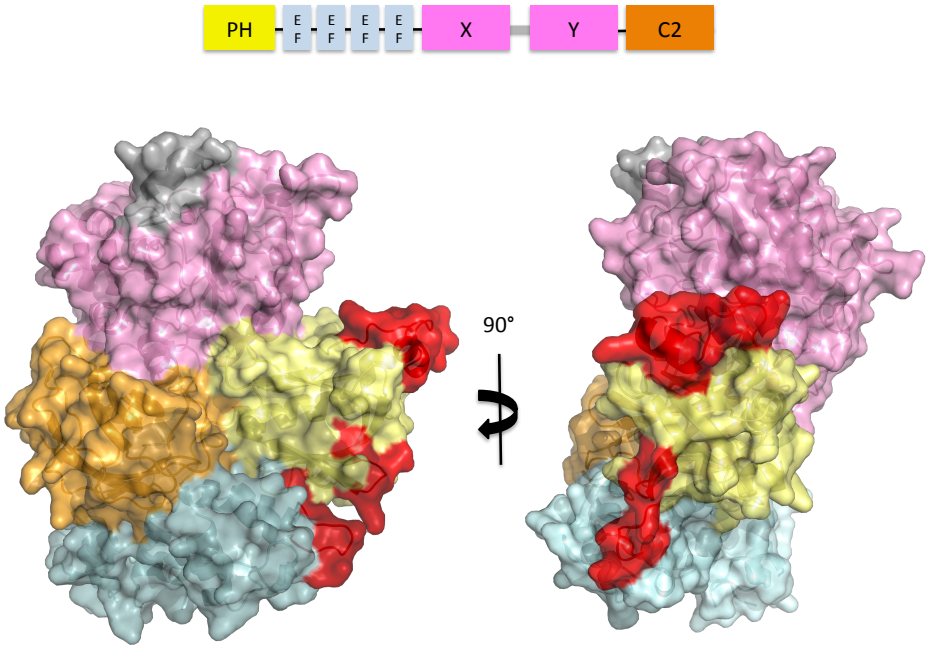

B)

Figure 2.1 General structure of PLCβ. A) Surface representation of PLCβ2 from 2FJU[25]. Colored surfaces correspond to the domain layout depicted above. Red surfaces indicate regions of the PH domain and the EF hands examined in this study. B) Sequence alignment of PLCβ3 and PLCβ4 in the region of the PH domain and first EF hand examined in this study. PLCβ3 sequences in bold denote loop substitutions for the corresponding sequences of PLCβ4. PLCβ3 loop deletion mutants were constructed by deleting these sequences in addition to the sequence underlined. Secondary structure elements are colored as in A. "*", ":" and "." denote positions in the alignment that correspond to full, strong and weak conservation respectively.

Materials and Methods

Sub-cloning, expression and purification of PLCβ proteins from mammalian cells

The coding sequence corresponding to human PLCβ3 (residues 11-847) was subcloned immediately downstream of a hexahistidine tag sequence located upstream of the multiple cloning site of pRK5 a CMV driven mammalian expression vector. Loop deletions and substitutions were generated using site-directed mutagenesis [61]. GST fusion proteins were constructed by subcloning DNA, encoding human PLCβ2 (residues 11-1180), into a modified pRK5 vector that includes a GST sequence upstream of the multiple cloning site.

HEK 293F cells were maintained in Freestyle Medium in a humidified environment, 6% CO_2 and vigorous shaking. Three days prior to the transfection, the cells were diluted in fresh medium to 0.5 x 10^6 cells/ ml. The day of the transfection the cells were harvested by centrifugation at 200 g for 5 min and resuspended in fresh medium to a final density between 2-2.5 x 10^6 cells/ml. The cells were then transfected using 25 kDa linear PEI (Polysciences, Inc.) at a 1:3 DNA:PEI ratio, as described previously [62,63]. Twenty-four hours later, the transfected cultures were diluted, two-fold, in fresh media and harvested the following day. The resulting cell pellets were washed with PBS prior to freezing in liquid nitrogen and stored at -80°C.

PLCβ proteins were purified by first thawing frozen cell pellets in room temperature lysis buffer consisting of 20 mM Bicine pH 7.6, 0.1% CHAPS, 100 mM NaCl, 0.1 mM EDTA, 0.1 mM EGTA, 2 mM DTT and 1X SigmaFast Protease inhibitors (ThermoFisher Scientific). This cells suspension was incubated at 4°C with gentle rocking. The lysate was then clarified by centrifugation for 15 min at 12,0000 X g. Prior to the addition of pre-equilibrated Ni-NTA affinity resin, the NaCl concentration of the clarified lysate was adjusted to 300 mM and further supplemented with 20 mM imidazole. After a 30-minute incubation, the resin was transferred to

a column and washed by gravity three times with 10 CV of wash buffer (20 mM HEPES pH 8, 300 mM NaCl, 20 mM imidazole, 0.1 mM EDTA, 0.1 mM EGTA and 2 mM DTT). Bound PLCβ was eluted by four separate additions of 2 CV of wash buffer supplemented with 150 mM imidazole. Purification of GST fusion proteins was performed using the same procedure with the following exceptions. Imidazole was omitted throughout, the concentration of HEPES in the wash buffer was adjusted to 100 mM, and GST fusion proteins were eluted using wash buffer supplemented with 10 mM reduced glutathione.

Expression and purification of human $G\beta_1\gamma_2$ from insect cells

Human $G\beta_1\gamma_2$, bearing a N-terminal hexahistidine tagged β subunit, was expressed in High Five cells, an insect cell line derived from the ovarian cells of the Trichoplusia ni, using a dual promoter insect cell expression vector described previously [51]. $G\beta_1\gamma_2$ was purified from membrane extracts of High Five cells harvested 48 hrs. post infection using Ni-NTA and anion exchange chromatography as described previously [64]. Fractions containing $G\beta_1\gamma_2$ were subsequently pooled and buffer exchanged into 20 mM HEPES pH 8.0, 100 mM NaCl, 0.5 mM EDTA, 2 mM $MgCl_2$ and 1 mM DTT using an S200 column. $G\beta_1\gamma_2$ containing fractions were then concentrated to 5 mg/mL, as determined by Bradford analysis, using a 30 kD cut-off Amicon Ultra-15 Centrifugal Filter Unit, flash frozen in liquid nitrogen, and stored at -80 ˚C until future use.

PLCβ activity assay

Basal activity and Gβγ mediated activation of PLCβ proteins was quantified using two different assay formats. One format has been described previously and based on measuring the

rate of hydrolysis of [^{3}H]-labeled PIP_2 in SUVs [65]. An alternative means of monitoring PLCβ activity was developed by adapting a TR-FRET based assay (Cisbio), consisting of an IP1-specific antibody conjugated to Terbium cryptate and d2-labeled IP1, as follows.

The SUVs were prepared by combining PE and PI (Avanti Polar Lipids) in a 1:0.4 molar ratio in a glass tube. The chloroform was evaporated from aliquots of this mixture using a nitrogen stream and the resulting film was dried for an additional hour to remove traces of solvent. The glass tubes were then sealed with parafilm and the dried lipids stored in a seal container at -20°C. The dried lipids were rehydrated as needed in assay buffer (50 mM HEPES pH 7.2, 3 mM EGTA, 80 mM KCl and 1 mM DTT) and sonicated for 5 min using a bath sonicator. The resulting 3X stock SUV solution has a final concentration of 750 μM PI and 300 μM PE.

Reactions were assembled on ice by combining SUVs, varying concentrations of Gβγ and 3 mM $CaCl_2$ in 0.2 ml PCR tubes. For measuring basal activity Gβγ was substituted with a blank solution such that all samples contained equal amounts of CHAPS. Prior to the addition of PLCβ, the reactions were transferred to a thermal cycler, pre-heated to 30°C, and incubated for 2 min. Reactions were initiated by adding 50 ng of PLCβ, diluted in assay buffer supplemented with 3 mg/ml BSA, for a final reaction volume of 12 μl. The reactions were quenched by adding 2 μl of 30 mM EGTA. Quenched reactions were then transferred to white, low volume 384 well plates and combined sequentially with 3 μl of d2-labeled IP and anti-IP1 antibody for a total sample volume of 20 μl. The plates were then sealed and incubated for 1 h prior to measurement of the fluorescence ratio of acceptor and donor emission signals (665 nm/620 nm) using a Flexstation5 plate reader (Molecular Devices).

Transfection of COS-7 cells and IP accumulation assay

COS-7 cells were maintained at 37°C in DMEM supplemented with 10% FBS in a humidified environment and 5% CO_2. The day prior to transfection, 12 well plates were seeded with COS-7 cells at a density of 1.2 x 10^5 cells/ well and incubated overnight. The following day, the cells were transfected with 200 ng of pRK5 PLCβ and 400 ng of pCI-Neo $G\beta_1$ and 400 ng of pCI-Neo $G\gamma_2$, or 800 ng of pRK5, and 2 ul of Lipofectamine 2000 (Life Technologies) per well. pCI-Neo $G\beta_1$ and pCI-Neo $G\gamma_2$ were generously supplied by Dr. A.V. Smrcka and constructed by subcloning the DNA sequences of human $G\beta_1$ bearing a N-terminal Avi-tag and bovine $G\gamma_2$ into the multiple cloning site of pCI-Neo (Promega). Transfected cells were incubated for 24 hrs. and then labeled overnight with [^{3}H] myo-inositol (3 μCi/ml) in F10 medium (Gibco).

The next morning, LiCl at a final concentration of 10 mM was added to each well. One hour later, the cells were washed with ice cold PBS and lysed by adding 1 ml of 50 mM formic acid. [^{3}H] IP was separated from cell extracts using 1 ml AG 1-X8 columns (Bio-rad). The columns were washed twice with 10 CV of 50 mM formic acid followed by 10 CV of 100 mM formic acid. Bound [^{3}H] IP was eluted with 3 ml of 1.2 M ammonium formate/100 mM formic acid combined with 10 ml of scintillation fluid. Scintillation counting was performed using a LS 6500 scintillation counter (Beckman)

GST pull down assay

Direct binding of PLCβ2 constructs to Gβγ was assessed by GST pull-down. Glutathione agarose beads (GoldBio) were pre-treated with PBS supplemented with 0.01% BSA to reduce non-specific binding. Samples consisted of 40 μl of glutathione agarose and 250 ul of one of the following: PBS, 50 nM GST-PLCβ2 or 50 nM GST-PLCβ2 in the presence of 25 ug of GST.

Each sample was incubated at 4°C with gentle rocking for 15 min before washing the agarose beads, three times, with 250 ul of DPBS to remove unbound proteins. Subsequently, the beads were incubated with 250 µl of 20 nM $G\beta_1\gamma_2$, diluted in PBS supplemented with 0.01% Lubrol, for 15 min at 4°C with gentle rocking. Unbound $G\beta_1\gamma_2$ was removed by washing the beads, three times, with 250 µl of PBS supplemented with 0.01% $C_{12}E_{10}$. Proteins bound to the agarose resin were eluted by addition of 1X Laemmli buffer directly to the beads and analyzed by western blot using a rabbit polyclonal $G\beta_1$ antibody (Santa Cruz Biotechnology).

Peptide array analysis of PLCβ PH domain – Gβγ interactions

Peptide arrays were synthesized using the SPOT method and the procedures described in [66]. Briefly, an automated peptide synthesizer was used to synthesize a series of overlapping peptides of varying lengths (12-15 amino acids) corresponding to the primary sequences of PLCβ3, residues (residues 1 – 847), and the PH domains of PLCδ1 (1-132), PLCβ1 (1-138), PLCβ2 (1-141) and PLCβ4 (1-135) onto derivatized cellulose membranes (Intavis). An additional series of overlapping peptides based on the sequences of SIRK (SIRKALNILGYPDYD) [67], QEHA (QEHAQEPERQYM-HIGTMVEFAYALVGK) [68], Gβγ binding sequences from the calcium channel Ca_V 2.2 (KSPLDAVLKRAATKKSRNDLI) [69] and GRK2 (WKKELRDAYREAQ-QLVQRVPKMKNKPRS) [70] as well as the epitope of the $G\beta_1$ antibody were synthesized in parallel and used as positive controls.

Post synthesis, the arrays were soaked in ethanol for five minutes and washed twice with deionized H_2O prior to incubation, at room temperature, in a blocking solution consisting of 5% non-fat dried milk in Tris buffered saline containing 0.1% Tween-20 (TBST). After the blocking step, the membranes were incubated at 4°C overnight in a 1-2 µM solution of $G\beta_1\gamma_1$ or $G\beta_1\gamma_2$

diluted in 20 mM HEPES pH 7.5, 100 mM NaCl, 10% glycerol, 0.8% octyl glucoside, 1 mM MgCl2, and 10 mM β-mercaptenol). Soluble $G\beta_1\gamma_2$ (C68S) was purified as described previously [51] and diluted in 20 mM HEPES pH 8, 100 mM, NaCl, 2 mM $MgCl_2$, 0.5 mM EDTA, 2 mM DTT. The following day, the membranes were washed three times with blocking solution prior to a 1 hr. incubation with a polyclonal rabbit antibody for $G\beta_1$ (Santa Cruz Biotechnology) at room temperature. Prior to incubating the membranes with an HRP-conjugated anti-rabbit antibody (1 hr. at room temperature) the membranes were washed three times with TBST. Following exposure to secondary antibody, the membranes were washed three times with TBST before addition of an enhanced chemiluminescent reagent and visualization using a Bio-Rad imager. The intensity of individual spots on a given array was determined using ImageJ software and represented as the average pixel intensity value per spot.

Results

Peptide array analysis of PLCβ PH – Gβγ interactions

While the isolated PH domains of PLCδ1 and PLCβ1-3 have been shown to bind directly to Gβγ [34], the specific residues that mediate the interaction have not been clearly defined. Peptide arrays have been employed successfully in the characterization of a number of protein-protein interactions [66,71] and provide a means of surveying the PH domains of PLCβ isozymes for common Gβγ binding motifs. Fig. 2.2 shows representative relative spot intensity plots for the PH domains of PLCδ1, PLCβ1, PLCβ2 and PLCβ4. Because regions that lie outside of the PLCβ PH domain have been reported to bind Gβγ our analysis also included a peptide array derived from the sequence of PLCβ3Δ847 (Fig. 2.3), a PLCβ3 truncation previously shown to include the minimal sequence required for Gβγ mediated activation [28].

Sequential spots on the array correspond to peptides of fifteen amino acids in length whose sequence is derived from the target sequences described above and an offset of three, resulting in an overlap of twelve amino acids between peptides synthesized on adjacent spots. Binding of the "prey" protein, Gβγ in this case, is expected to produce spot intensities that generally converge around a single spot. In these experiments, there were no distinct spot clusters. This result could be due an inherent inability of the synthesized peptides to recapitulate the native interaction between PH domain and Gβγ, which is likely modulated by lipid membranes that are not present in this experiment. More likely, it could indicate that residues distant from each other in the primary sequence of PLCβ are brought closer together in the folded enzyme to form the Gβγ binding site. Similar results from those presented in Figure 2.3 were obtained using geranylgeranylated Gβγ subunits indicating that the lipid modification had no effect on the affinity of the synthesized peptides toward Gβγ under these conditions.

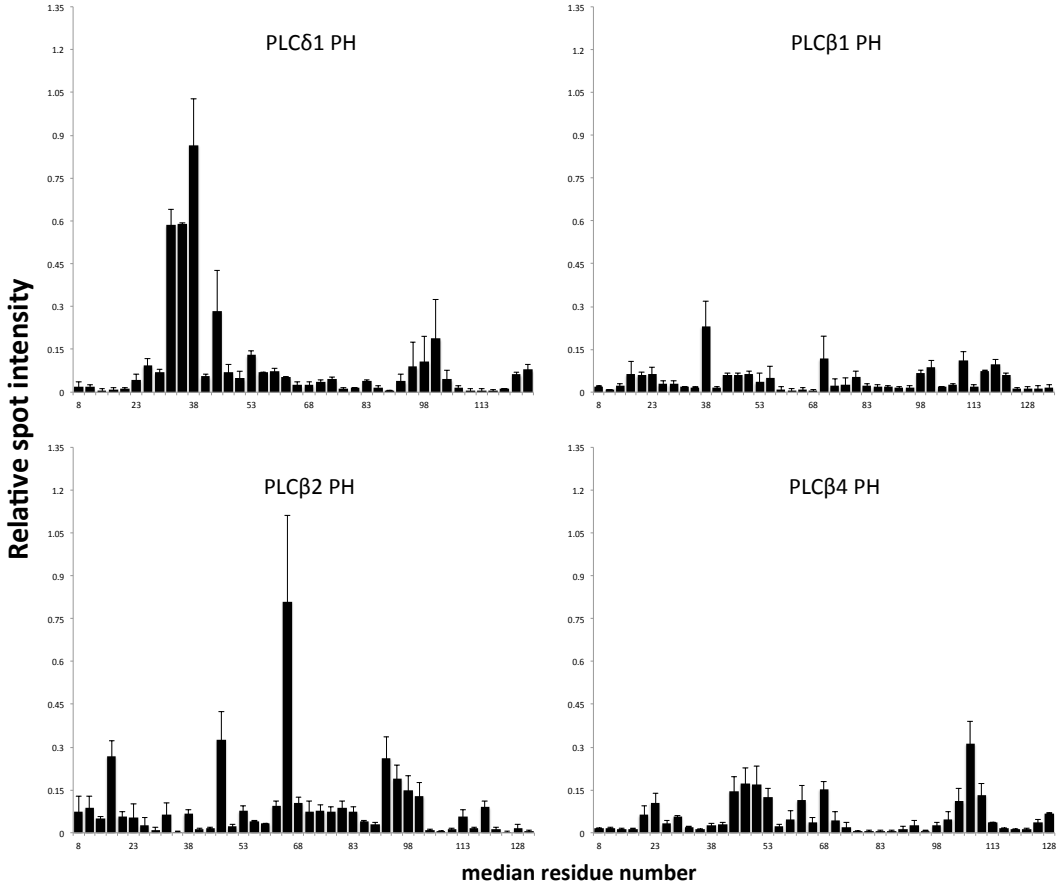

Figure 2.2. Far western analysis of PLC PH-Gβγ interactions. Peptide arrays derived from the sequences of several PLC PH domains were synthesized directly onto a derivatized cellulose membrane and probed with 1 μM $G\beta_1\gamma_2$C68S. Data presented here represent average spot intensities from two separate arrays relative to a control peptide (AASIRKALNILGYPD) derived from SIRK.

A)

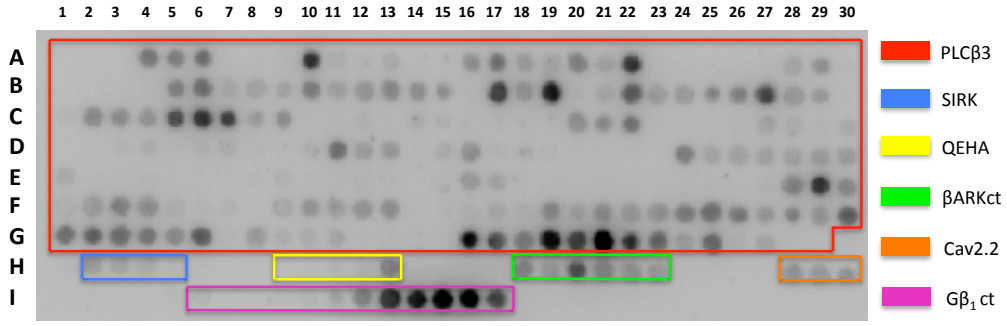

B)

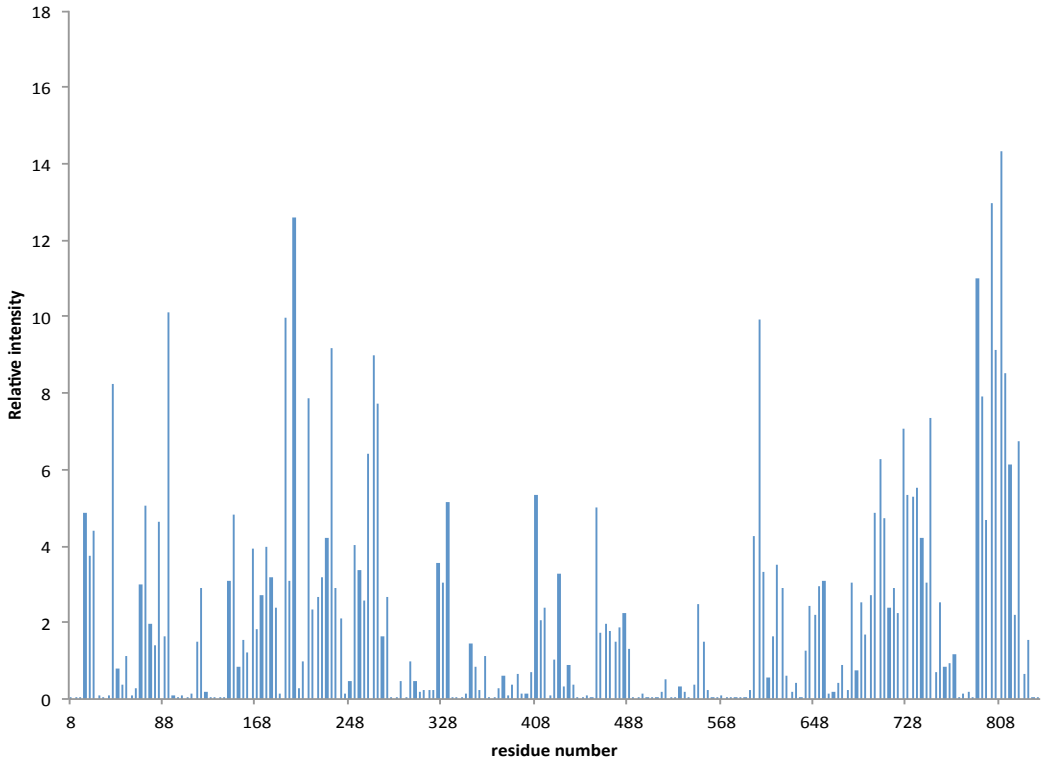

Figure 2.3. PLCβ3 peptide array screening for Gβγ interaction sites. A. A series of peptides with sequences that match overlapping segments of PLCβ3Δ847 (red outline) were synthesized directly onto derivatized cellulose using the SPOT method. The raw image shown here is from one such array treated with 0.4 μM $G\beta_1\gamma_1$ as described in the Materials and Methods section. Additional overlapping peptides derived from SIRK, QEHA, Cav2.2, βARKct and the epitope used to generate the $G\beta_1$ antibody (blue, yellow, green, orange and magenta outlines respectively) are included as positive controls. B. Relative spot intensities for the array presented in A. The x-axis corresponds to the residue number of PLCβ3Δ847 that matches the median amino acid of a given peptide within the array.

Sequence substitution of solvent exposed loops near the PLCβ-Rac interface for those of a Gβγ insensitive isoform does not alter Gβγ responsiveness

We next examined the crystal structures of PLCβ2 bound to Rac1 and PLCβ3 bound to $G\alpha_q$ (PDB entries 2FJU and 4GNK, respectively) and observed that adjoining loops from the PH domain and EF hand motifs, β3/β4 from the PH domain and α1/α2 of the EF hand contribute to a unique protein-protein interface present in both crystal structures (Fig. 2.4). We hypothesized that these could potentially contact Gβγ, consistent with reports suggesting that regions from the EF hands might also contribute to interactions with Gβγ [72]. As seen in figure 2.5A, substitution of residues 55-60 (PH_Lβ3/4) from the PH domain and 164-169 from the first EF hand (EF_Lβ3/4) of PLCβ3 for the corresponding sequences from the Gβγ insensitive isoform PLCβ4 had no effect on the responsiveness of these chimeric proteins to Gβγ. Similar results were obtained when using IP accumulation assays in COS-7 cells transiently transfected with plasmids encoding PLCβ3 and Gβγ (Fig. 2.5B)

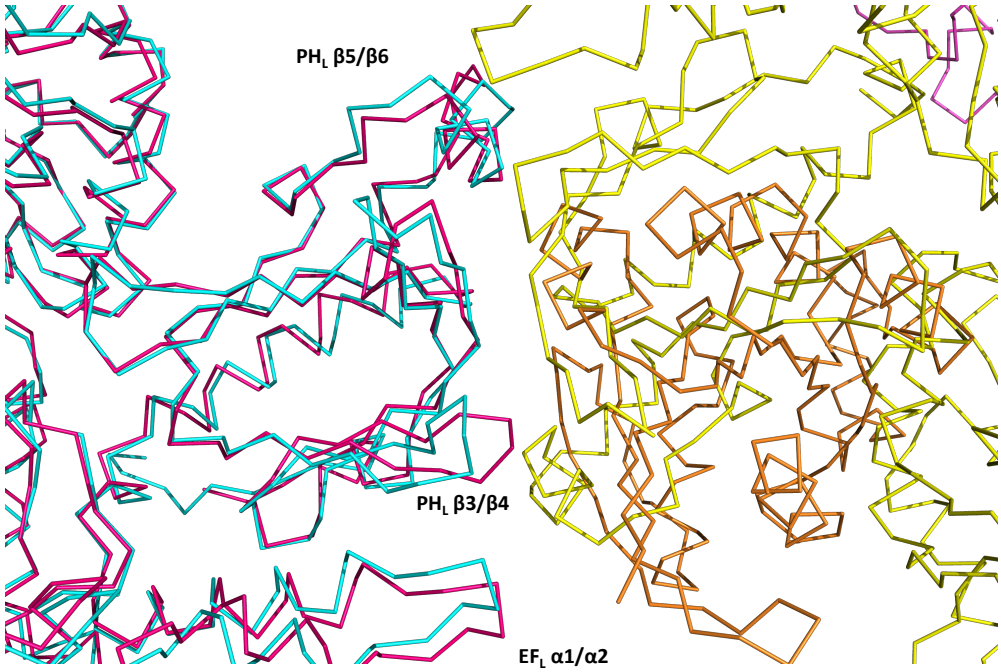

Figure 2.4 Overlay of PLCβ structures reveals potential protein-protein interface. Superimposition of the structures of PLCβ2 (magenta) bound to Rac1 (orange) (PDB ID: 2FJU) and PLCβ3 (cyan and yellow) bound to $G\alpha_q$ (PDB ID: 4GNK) centered on the PH domain-Rac1 interface.

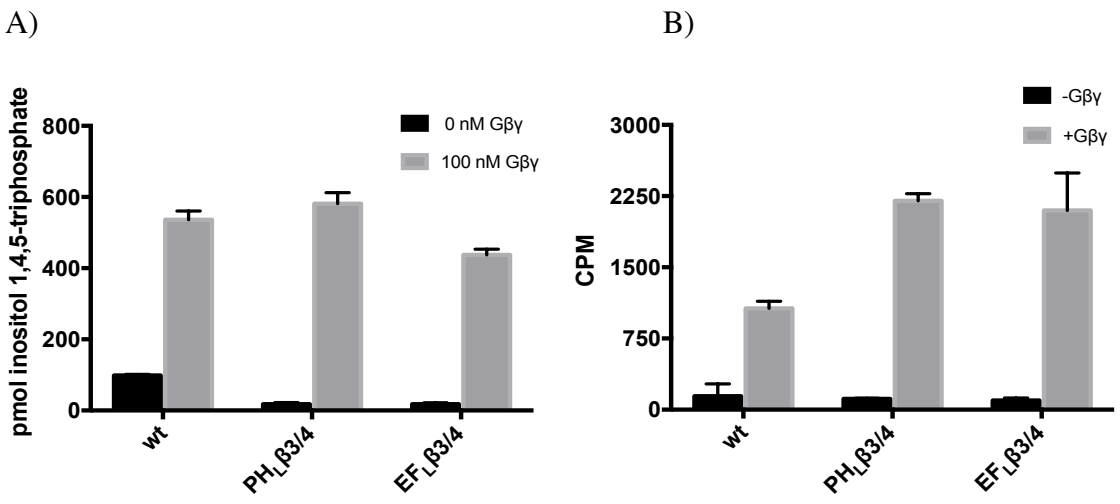

Figure 2.5. Effect of PH and EF loop substitutions on Gβγ responsiveness of PLCβ3. A. The activity of PLCβ3Δ847 and variants in which the loops connecting strands β3 and β4 of the PH domain (PH_Lβ3/4) and helices α1 and α2 of the adjoining EF hand (EF_Lβ3/4) cells were substituted with the corresponding sequences from PLCβ4 was measured in the presence (gray bars) and absence (black bars) of 100 nM $G\beta_1\gamma_2$ using SUVs containing [^{3}H]-PIP2 as described in Materials and Methods. B. COS-7 cells were transiently transfected with DNA encoding the same PLCβ3 constructs as in A and plasmid DNA encoding $G\beta_1$ and $G\gamma_2$ subunits (gray bars) or pRK5 (black bars)**.**

Deletion of solvent exposed loops ablates Gβγ mediated activation

In addition to examining the effects of substitution of the aforementioned loops, we generated a series of loop deletion mutants and evaluated their responsiveness to Gβγ. As shown in figure 2.6A, deletion of the loops connecting β-strands 3 and 4 and β-strands 5 and 6 of the PH domain in addition to the loop connecting α-helices 1 and 2 of the adjacent EF hand motif led to a loss of Gβγ mediated activation. Importantly, deletion of these solvent exposed loops does not disrupt the ability of PLCβ to hydrolyze PIP2 in the absence of Gβγ (Fig. 2.6B). These effects were recapitulated in COS-7 cells transiently co-transfected with PLCβ3 and $G\beta_1\gamma_2$ DNA (Fig. 2.6C).

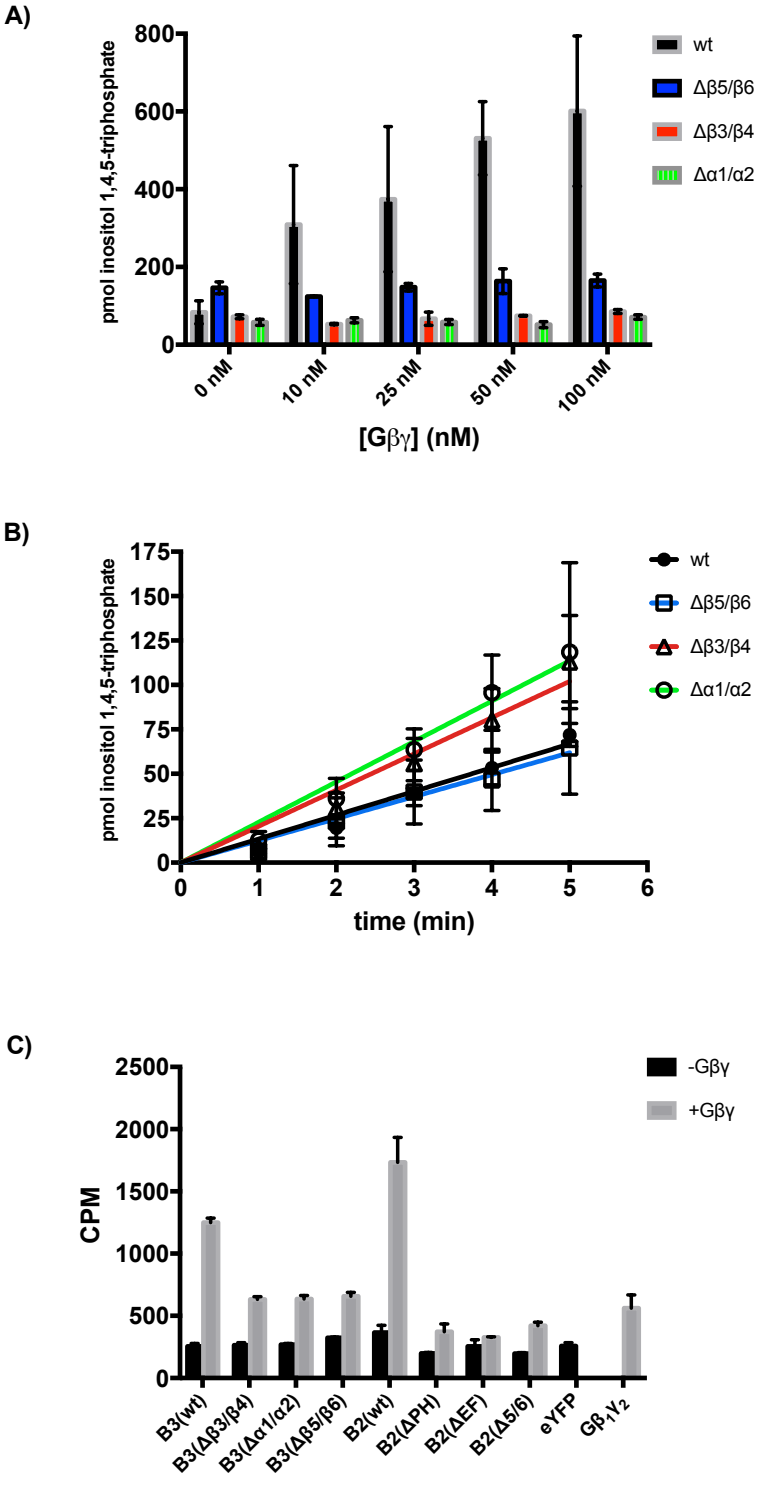

Figure 2.6 Deletion of solvent exposed loops of the PH domain and adjacent EF hands reduces Gβγ responsiveness. A. Gβγ mediated activation of wild-type PLCβ3Δ847, and loop deletion mutants Δβ5/β6 (residues 81-97), Δβ3/β4 (residues 55-60) and Δα1/α2 (residues 164-169) was measured using SUVs containing [^{3}H]-PIP2 as described in the Materials and Methods section using increasing concentrations of $G\beta_1\gamma_2$. B. The basal activity was determined by measuring the amount of product formed, as in A, at different time intervals. C. IP accumulation in response to exogenously expressed Gβγ was measured in COS-7 cells labeled with [^{3}H]-myo-inositol by transient transfection of PLCβ3Δ847 (B3) or GST-PLCβ2 (B2) and their respective loop deletion variants, denoted in parenthesis. PLCβ plasmids were cotransfected with DNA encoding $G\beta_1$ and $G\gamma_2$ (gray bars) or pRK5 (black bars). Mock transfections with pEYFP and Gβ1γ2 were included to account for endogenous PLCβ activity. Data in A and B represent average of two experiments performed in duplicate ± SEM. Data in C represents a single experiment performed in duplicate.

Effector binding to PLCβ is thought to relieve auto-inhibition via interfacial activation or optimization of the orientation of the active site relative to the membrane [73,74]. Whether direct binding of Gβγ to the PH domain would be conducive to activation by this generalized mechanism is still unknown. Notably, binding of the PLCβ PH domain to membranes has been reported to alter the relative orientation of the TIM barrel [75]. To determine if the observed loss of responsiveness of the loop deletion mutants was a direct consequence of an ablation of Gβγ binding, we evaluated direct binding of a series of GST-PLCβ2 fusion proteins bearing the equivalent deletions as the PLCβ3 variants. These constructs were chosen over their PLCβ3 counterparts because their yield in HEK293F were higher, they could be purified to near homogeneity and their Gβγ response mirrored that of the PLCβ3 variants in COS-7 cells (Fig. 2.6C). Figure 2.7 shows that all three loop deletion mutants are still able to bind to Gβγ suggesting that while these loops are critical for activation they are not necessary for Gβγ binding.

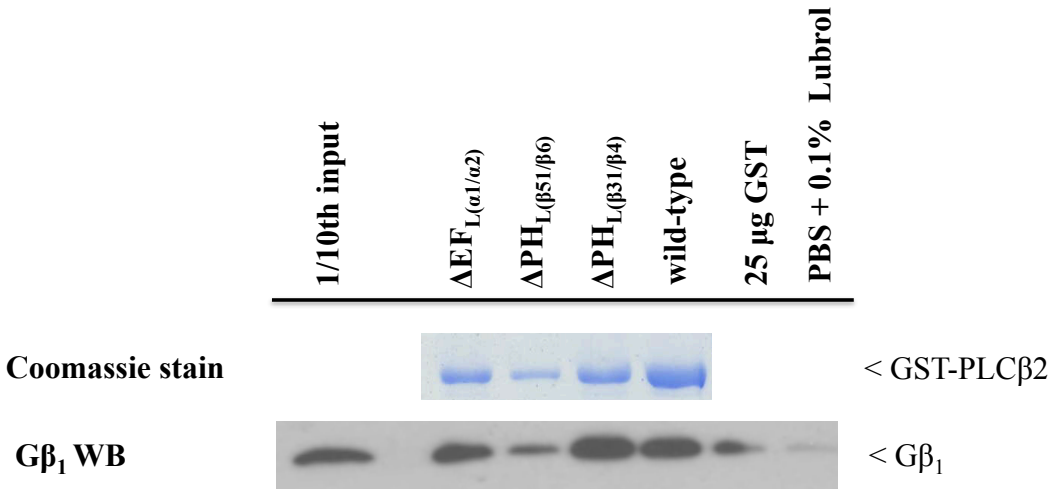

Figure 2.7. Binding of Gβγ to PLCβ2 loop deletion mutants by GST pulldown. Loop deletion mutants $\Delta EF_{L(\alpha1/\alpha2)}$ (residues 50-55), $\Delta PH_{L(\beta5/\beta6)}$ (residues 76-93), $\Delta PH_{L(\alpha1/\alpha2)}$ (residues 159-164), wild-type GST-PLCβ2 and 25 µg of GST were bound to glutathione agarose beads, incubated with $G\beta_1\gamma_2$ and subsequently washed prior to elution with sample buffer. Eluted proteins were analyzed by SDS-PAGE, transferred onto a PVDF membrane and probed with a $G\beta_1$ primary antibody.

TR-FRET assay for the quantification PLCβ activity

During the course of this study, an alternative to the standard radiometric PLC activity assay [65] was developed because the substrate, H^3-PIP2, was no longer commercially available. Based on the observation that all eukaryotic PLC isozymes are able to catalyze the hydrolysis of PI, PIP, and PIP2 in vitro [76–78], we reasoned that a commercial HTRF based assay, originally developed by Cisbio for the investigation of $G_{q/11}$ signaling pathways from cellular extracts, could be easily adapted for the quantification of IP generated by the catalytic activity of PLCβ in a reconstituted system (Fig. 2.8).

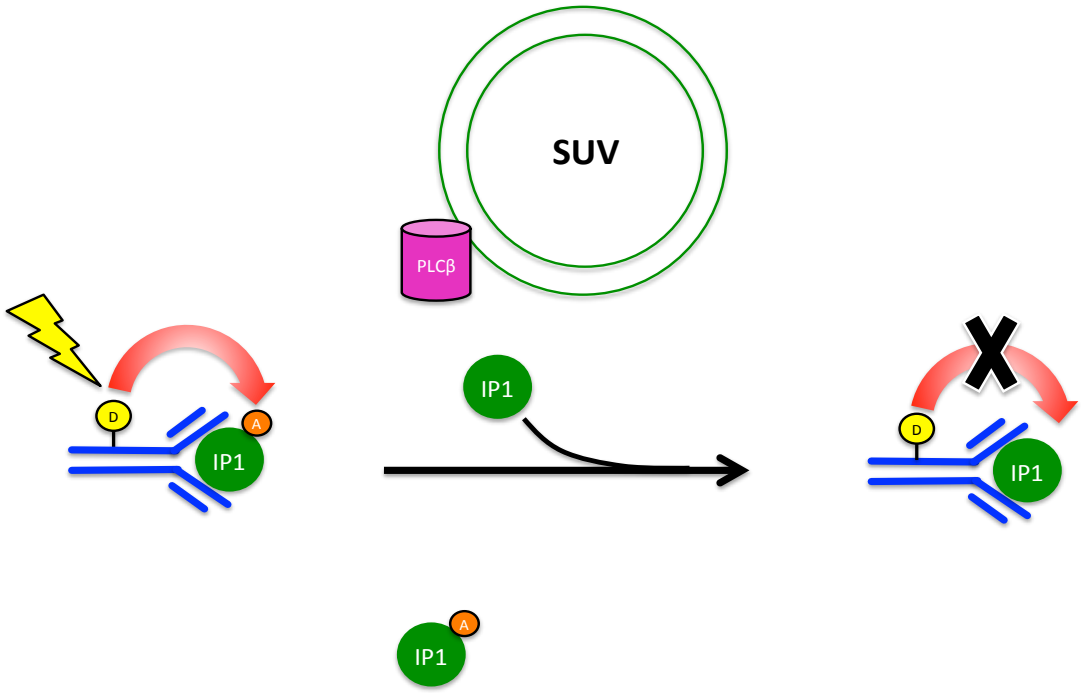

Figure 2.8 TR-FRET assay for measuring PLC activity. The assay relies on FRET between an IP1-specific antibody conjugated to a donor molecule and d2labeled IP1. Competitive displacement of the d2-labeled IP1 by the IP generated by the PLCβ-catalyzed hydrolysis of PI in SUVs comprised of PE and PI results in a quantifiable decrease in the FRET signal.

The assay was initially characterized by determining its dynamic range using an IP1 standard included with the commercial kit. As presented in figure 2.9, our experimental set up allowed for the reliable detection of IP1 in the approximate range of 30 nM to 300 nM.

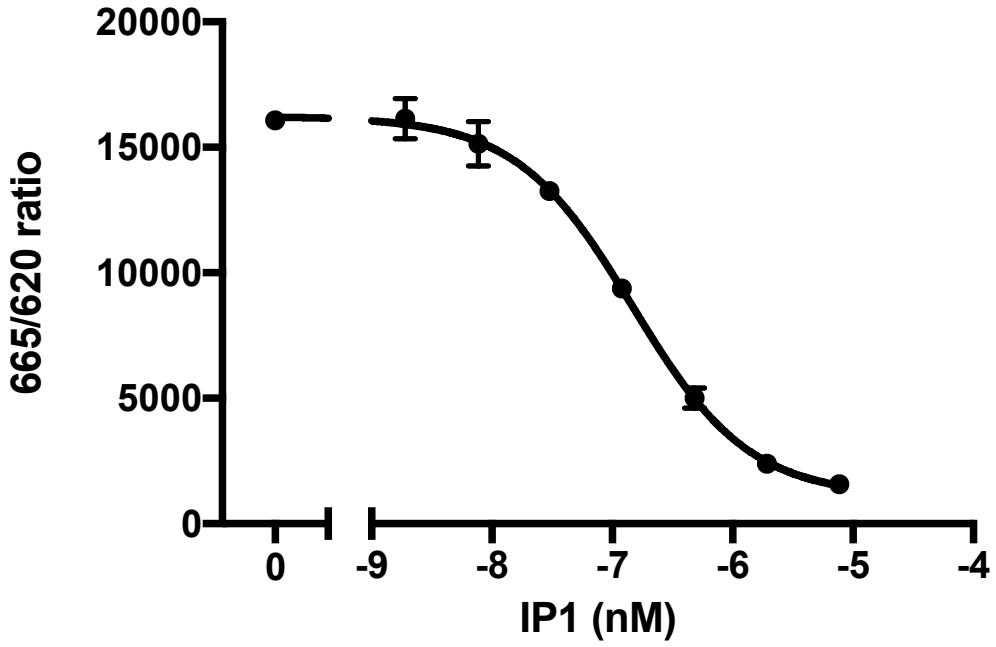

Figure 2.9. Dynamic range of Cisbio IP-One assay. A dilution series of IP1 standards was prepared as per manufacturers recommendations. The fluorescence emission at 665 and 620 nm of samples containing a single concentration of IP1, the IP1 antibody and d2-labeled IP1 was measured using a Flexstation 5 plate reader and plotted as the ratio of emissions (665/620) x 10000. Data represent two individual experiments performed in triplicate ± SEM.

We then determined if indeed the assay could be used to monitor the activity of PLCβ isozymes. Figure 2.10 shows that both basal activity and Gβγ response of PLCβ3 is quantifiable using the aforementioned HTRF assay. Notably, the rate of PLCβ2-catalyzed hydrolysis of PI in SUVs has been estimated previously as 26.9 nmol/min/mg PLCβ2 [78]. Based on the plots depicted in figure. 2.10, basal activity of PLCβ3 using present is approximately 7 nmol/min/mg. Whether this difference can be accounted for by differences in assay format, reaction temperature, SUV composition or simply a reflection of isoform specific PLCβ activities are unclear at the moment and will require additional testing. The parity in basal activities between wild-type and the Δ847 variant is unexpected since previous studies have shown than truncation of the CTD reduces membrane association of PLCβ [79] which in turn result lower activity. The end point estimate of activity of wild-type and Δ847 in the absence of Gβγ (Fig. 2.10 B and D) that indicate the wild-

type enzyme is more active. Notably, these estimates for the activity of wild-type enzyme are derived from a single experiment and necessitate further validation.

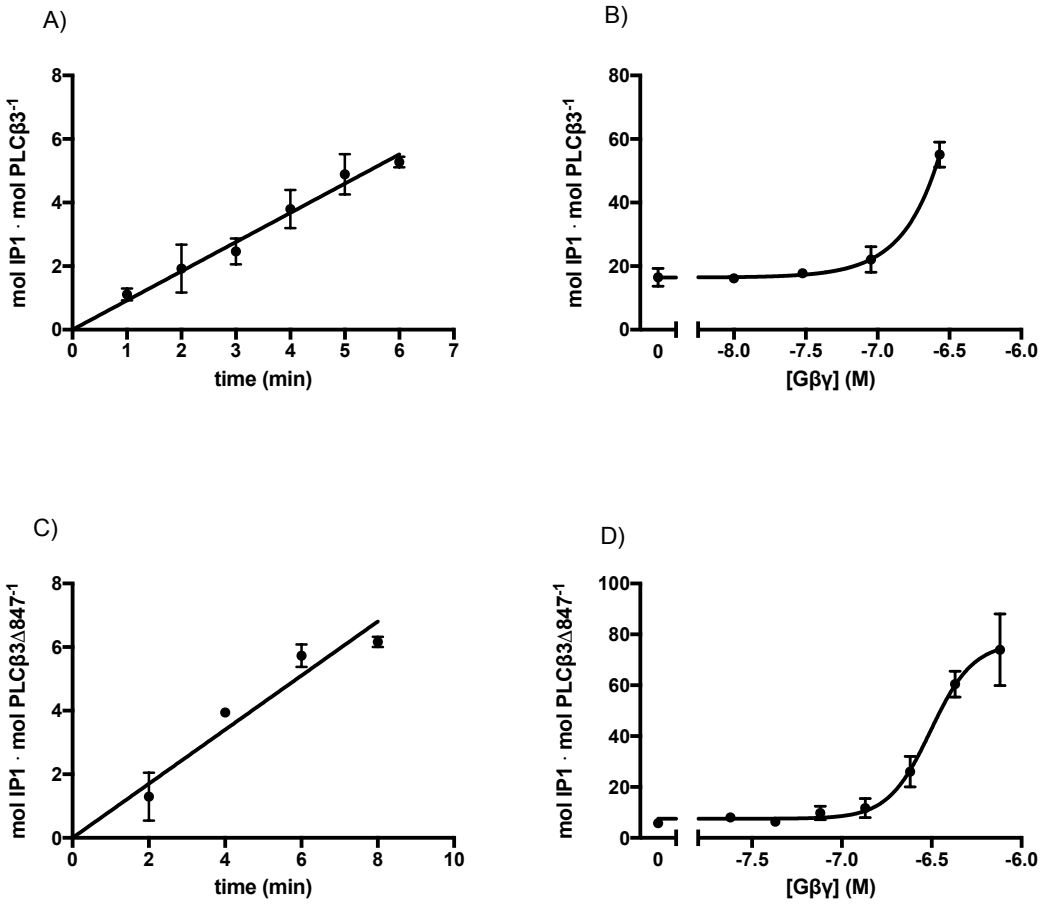

Figure 2.10. Quantification of PLCβ3 basal and Gβγ stimulated activities. The TR-FRET assay was used to determine the basal activity (A and C) and Gβγ response (B and D) of full-length PLCβ3 and the C-terminal truncation variant used in this study. Data in A and B represent average values ± SEM of duplicate reactions from a single experiment. Data in C and D represent average values ± SEM of at least two independent experiments.

Discussion

The affinity of isolated PH domains towards Gβγ, its recurrence in other Gβγ effectors, such as GRK2 subfamily members, and the feasibility of modulating responsiveness by swapping the PH domains of sensitive and insensitive PLC isoforms provide strong support for

the PH domain in mediating Gβγ responsiveness. Whether direct binding of Gβγ to the PH domain in the context of the intact enzyme is crucial for activation of PLCβ however remains unclear. Using mutational analysis, we examined the contributions of several solvent exposed loops of the PH/Rac1 interface in mediating Gβγ stimulated activity of PLCβ. Our findings suggest that although these loops are important for Gβγ mediated activation of PLCβ isozymes they are dispensable for the interaction with Gβγ.

The observation that substitution of the β3-β4 loop of the PH domain and α1-α2 loop of the adjoining EF hand for the corresponding sequences in PLCβ4 had no effect on Gβγ responsiveness is consistent with our peptide array data, which suggest that the Gβγ binding site of PLCβ is not likely contained within a short span of contiguous residues. Notably, the spot intensities for peptides derived from the Tα5 helix of the TIM barrel (residues 621-633 of PLCβ3), previously identified as a putative Gβγ binding site [80], were not consistent with direct binding of Gβγ to this region. Whether the lack of direct binding is a consequence of differences in experimental approach are unclear. Given that no complex between PLCβ and Gβγ can be formed by size exclusion chromatography (data not shown), the interaction is presumably weak in the absence of lipid bilayers, which could also account for the lack of detection in our peptide array analysis. The loops examined in this study are represented on the peptide array shown in figure 2.3A by spots A12-A15 (β3-β4), A19-A22 (β5-β6) and B9-B12 (α1-α2). Although some individual spots along this range are observable the lack of spot clusters in these regions of suggest that these loops Gβγ directly.

The effects of deletion of the β5-β6 loop observed in the present study are consistent with a previous report where mutation of basic residues along this loop led to diminished responsiveness to Gβγ [75]. The authors of this report propose that, in solution, the PLCβ PH

domain contacts conserved regions of the Y domain and that this interaction is inhibitory. Membrane association and Gβγ binding are purported to disrupt these inhibitory interactions and stabilize an active state of the enzyme. Further refinement of this model suggests that residues on the β5-β6 loop (residues 71-96) form part of the Gβγ-PH domain interface [37]. Concurrent mutation of residues Pro90 and Asp91 (P90I/D91G) of the PLCβ2/δ1 chimera described previously, led to a reduction in Gβγ response, nearly six-fold compared to wild-type, despite FRET measurements of fluorescently-labeled PLCβ2 chimera indicating direct binding to Gβγ. Disruption of both direct binding of Gβγ, as indicated by FRET measurement and hydrolysis of PIP2 was apparent only upon mutation of a third residue Lys71 (P90I/D91G/K71A). Notably, the effects of deletion of residues 81-97 described here are consistent with those reported for the P90I/D91G mutant. Indeed, our cumulative results suggest that while perturbations of this loop affect Gβγ activation of PLCβ, these residues are unlikely to contact Gβγ directly.

Recently, Kadamur et al [35] have proposed a similar model in which reorientation of the PH domain leads the exposure a Gβγ binding site buried within the PH/EF interface observed in the crystal structures of PLCβ. The hypothetical Gβγ binding surface was surmised on sequence alignment of the PH domains of PLCβ and GRK2 and the application of chemical crosslinking to constrict the presumed motions of the PH domain. Regions of the first EF hands have been implicated previously in Gβγ mediated activation of PLCβ isozymes [72,75,81]. Our results suggest that the solvent exposed loops that form the PH/EF interface are dispensable for the interaction of PLCβ with Gβγ because their deletion did not disrupt Gβγ binding.

In summary, our results indicate that the solvent exposed loops used to form the PH/Rac1 interface in PLCβ2 are unlikely to mediate direct interactions of Gβγ-responsive PLCβ isoforms.

The observation that deletion of any of these loops preserves basal activity indicates that they do not suffer from gross folding defects. Deletion of these loops did not ablate Gβγ binding; suggesting that they might be critical in aligning the membrane-binding sites of Gβγ and PLCβ in a manner that is conducive to enhanced hydrolysis of PIP2. Importantly, our results do not rule out the existence of a Gβγ binding site on any surface, buried or otherwise, of the PLCβ PH domain but rather highlight its importance beyond that of a mediator of protein-protein interactions in the regulation of PLCβ by Gβγ.

Additionally, we demonstrate that a pre-existing HTRF assay used for assessment of PLCβ activity in cell lysates could be adapted for the determination basal and Gβγ mediated activity of PLCβ. Although a more detailed characterization is needed to assess the applicability of this new format to the study other PLC isoforms, in its current state it offers several advantages over the conventional radiometric assay which include the exclusion of radioactive materials, an amenability to miniaturization and the potential of adapting the same assay format for the evaluation PLC activity in cells. More importantly, this new format could vastly increase the speed at which we screen PLCβ variants and thus expedite our understanding of its function.

CHAPTER 3

FUNCTIONAL ANALYSIS OF THE GRK2-Gβγ COMPLEX: EFFECTS OF THE LIPID COMPOSITION AND SMALL MOLECULE INHIBITION[1]

Introduction

The activity of GRK2, perhaps best known for its ability to initiate the desensitization of active GPCRs, is also regulated by Gβγ [82]. This function necessitates localization to the plasma membrane and most GRK subfamilies have evolved to include a C terminal lipid modification that anchors them to the membrane. Members of the GRK2 subfamily, however, possess no such modification but rather rely on interactions between its PH domain and Gβγ for membrane targeting [46]. The PH domain of GRK2 subfamily members also binds PIP2, and this interaction has been shown previously to be important for GRK2 activity [83,84]. How the concerted binding of Gβγ and PIP2 modulate the activity of GRK2 is not evident from the available structural data since neither Gβγ nor the inclusion of IP3, a surrogate for the head group of PIP2, promotes large conformational changes in GRK2 [54].

[1] The data presented in this chapter, which is published elsewhere[88,91103], is not solely my work but the result of collaborative efforts. My contributions included the purification of both GRK2 and $G\beta_1\gamma_2$, the preparation of GRK2-Gβγ complexes used in spectroscopic determination of membrane orientation and the structure determination (including crystal growth and harvest, diffraction experiment, data collection, and model building and refinement) of the co-crystal structure of 14as bound to the GRK2-Gβγ complex.

Once recruited to the membrane, the activity of GRKs is likely influenced by the orientation of their active site relative to their membrane-bound native substrates; active GPCRs [85]. Importantly, the structural analysis of the GRK2-Gβγ complex cannot, by its very nature, account for how these two regulatory inputs, binding to Gβγ and PIP2, might affect the orientation of GRK2 on the membrane. Sum frequency generation (SFG) vibrational spectroscopy provides a means of examining such effects and has been applied previously to investigate how proximity to membrane lipids might influence the orientation of both Gβγ and the GRK2-Gβγ complex[55,86]. These studies revealed that the orientation of Gβγ, relative to the membrane, is altered upon binding to GRK2 such that the receptor-binding site of the kinase is poised to engage activated GPCRs.

Subsequent studies successfully combined SFG measurements with those of a complementary technique, attenuated total reflectance–Fourier transform infrared (ATR-FTIR) spectroscopy, allowing for a more accurate estimation of membrane orientation as a result of limiting the number of possible orientations predicted by SFG measurements alone[87]. We have applied this combined vibrational spectroscopy approach to study the effects of membrane lipid composition on the orientation of the GRK2-Gβγ complex revealing that membranes containing PIP2 induce an orientation of the GRK2-Gβγ complex that positions the receptor-docking site of GRK2 in close proximity to the surface of the membrane[88].

General interest in GRK2 clearly extends beyond its regulation by Gβγ subunits. Upregulation of GRK2 in cardiac failure is known to impair the normal function of the β-adrenergic receptor and several studies have shown that blocking the activity of GRK2 can partially restore the responsiveness of the receptor towards catecholamines leading to improved heart function [89]. The merits of GRK2 as a therapeutic target have been explored extensively and

these efforts have led to the development of several strategies that vary in both potency and efficacy [50]. The crystal structures of two such inhibitors, Takeda CMPD103A (**1**) and TakedaCMPD101 (**2**) (Fig.3.1), bound to the GRK2-Gβγ complex were solved previously in the lab in order to define the structural basis of their action [90].

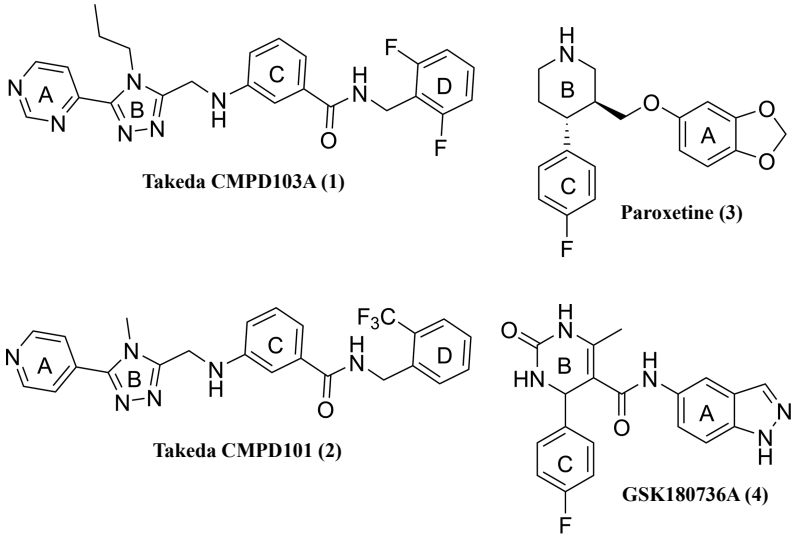

Figure 3.1. Chemical structures of known GRK2 inhibitors. The ring systems of all four structures are labeled to denote the subsites (A for ribose, B for adenine, C for pyrophosphate and D for hydrophobic subsites respectively) occupied by each inhibitor within the active site of GRK2.

As revealed by these structures, both inhibitors occupy four distinct subsites within the ATP binding pocket (Fig. 3.2A). Subsequent structure determination of analogous complexes in the presence of paroxetine, an FDA approved serotonin re-uptake inhibitor with modest potency, and GSK180736A, a structurally similar yet slightly more potent GRK2 inhibitor, revealed that unlike the Takeda compounds, neither compound occupies the hydrophobic subsite within the GRK2 active site (Fig. 3.2B). This observation prompted the development of several hybrids of Takeda103A and GSK180736A in order to combine the enhanced potency of the first and the more favorable pharmacokinetic properties of the latter[51].

More recently our efforts have focused on extending this hybrid strategy to the paroxetine scaffold in order to produce selective and potent GRK2 inhibitors with improved drug-like properties relative to the more potent Takeda compounds[91]. The strategy implemented here progressed through the appendage of amide moieties to the fluorophenyl ring of paroxetine leading to the successful design of several compounds including 14as, our most potent and selective inhibitor to date, bound to GRK2-Gβγ. As described below, this structure reveals the basis for the increased potency of 14as, relative to its parent scaffold, and provides further support for the validity for the structure-based development potent and selective GRK2 inhibitors.

A)

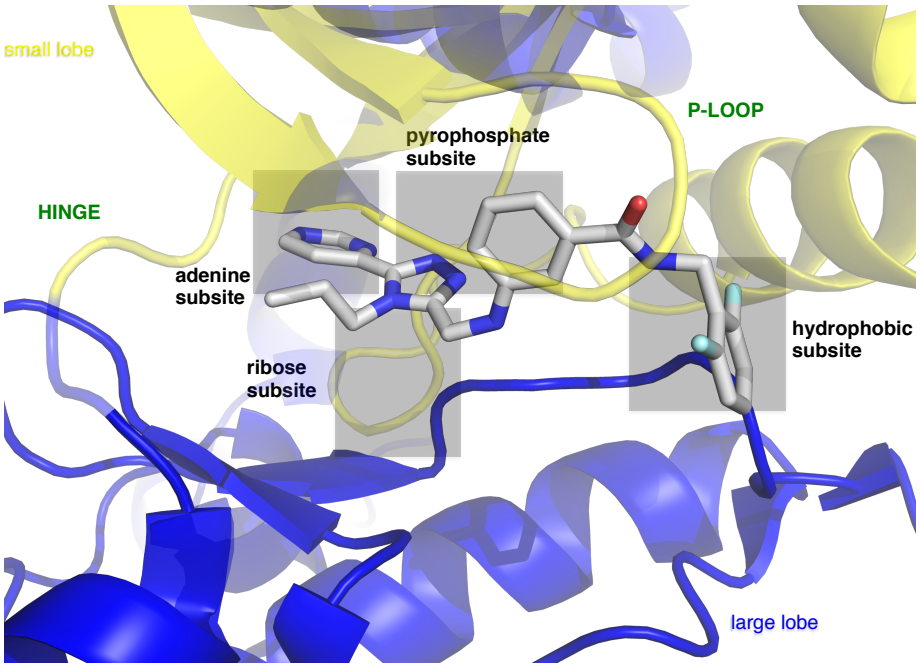

B)

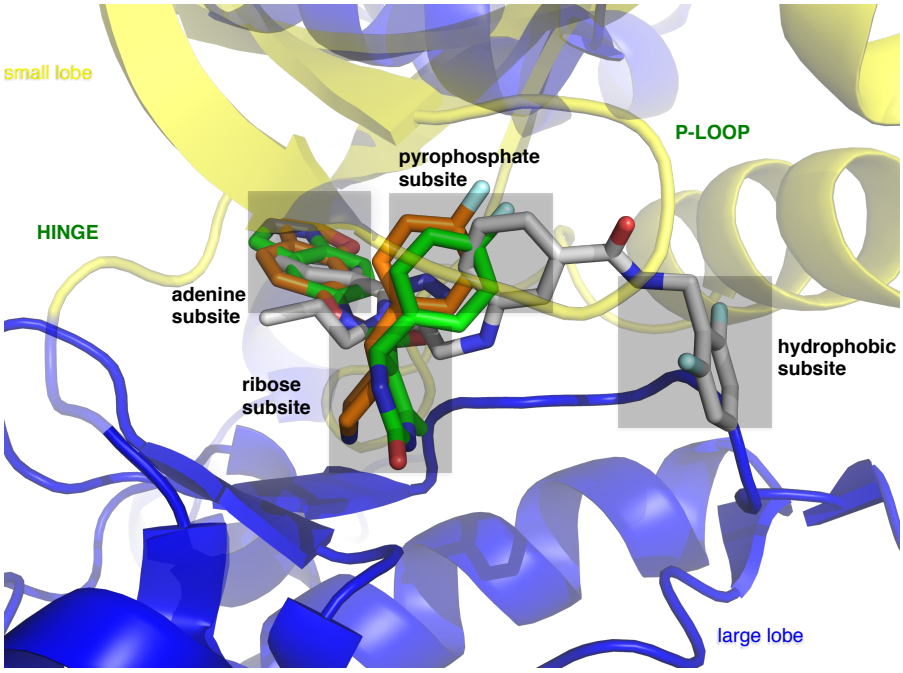

Figure 3.2. Crystal structures of known GRK2 inhibitors. A. Active site view from 3PVW, the co-crystal structure of **1** (gray stick representation) bound to GRK2-Gβγ[90], how this inhibitor occupies all four subsites within the active site of GRK2. Both small and large lobes (colored yellow and blue respectively) contribute to the overall structure of the active site and harbor residues that contact **1** B. Overlay of the structures of **1** (gray), **3** (orange) and **4** (green) from 3PVW[90], 3V5W[92] and 4PNK[93] respectively. The view is the same as in A and shows how both **3** and **4** do not extend into the hydrophobic subsite.

Material and Methods

Expression and purification of GRK2 and $G\beta_1\gamma_2$ complexes for SFG and ATR-FTIR spectroscopy

The S670A mutant of full length bovine GRK2 bearing a C-terminal hexahistidine tag was expressed in High Five cells using the Bac to Bac insect cell expression system (Life Technologies) and harvested 48 h post-infection. GRK2 was purified from clarified lysates using Ni-NTA affinity resin and cation exchange chromatography as described previously[94] and subsequently gel filtered into 20 mM HEPES pH 7.5, 100 mM NaCl, and 1 mM DTT using a Sephadex 200 (S200) column (Fig. 3.3A).

Human $G\beta_1\gamma_2$ containing an N-terminally hexahistidine-tagged β subunit was expressed using a dual promoter insect cell expression vector (a gift from Dr. Brian Kobilka) in High Five cells and harvested 48 h post-infection. $G\beta_1\gamma_2$ was purified from clarified lysates using Ni-NTA affinity resin and anion exchange chromatography as described previously[51] (Fig. 3.3B) and stored at −80 °C until further use. GRK2-Gβγ complexes were prepared by combining each protein in a 1:1 molar ratio and diluting the resulting complexes in a buffer consisting of 20 mM HEPES (pH 8.0), 50 mM NaCl, 1 mM CHAPS and 5 mM DTT prior to their use SFG and ATR-FTIR spectroscopy experiments.

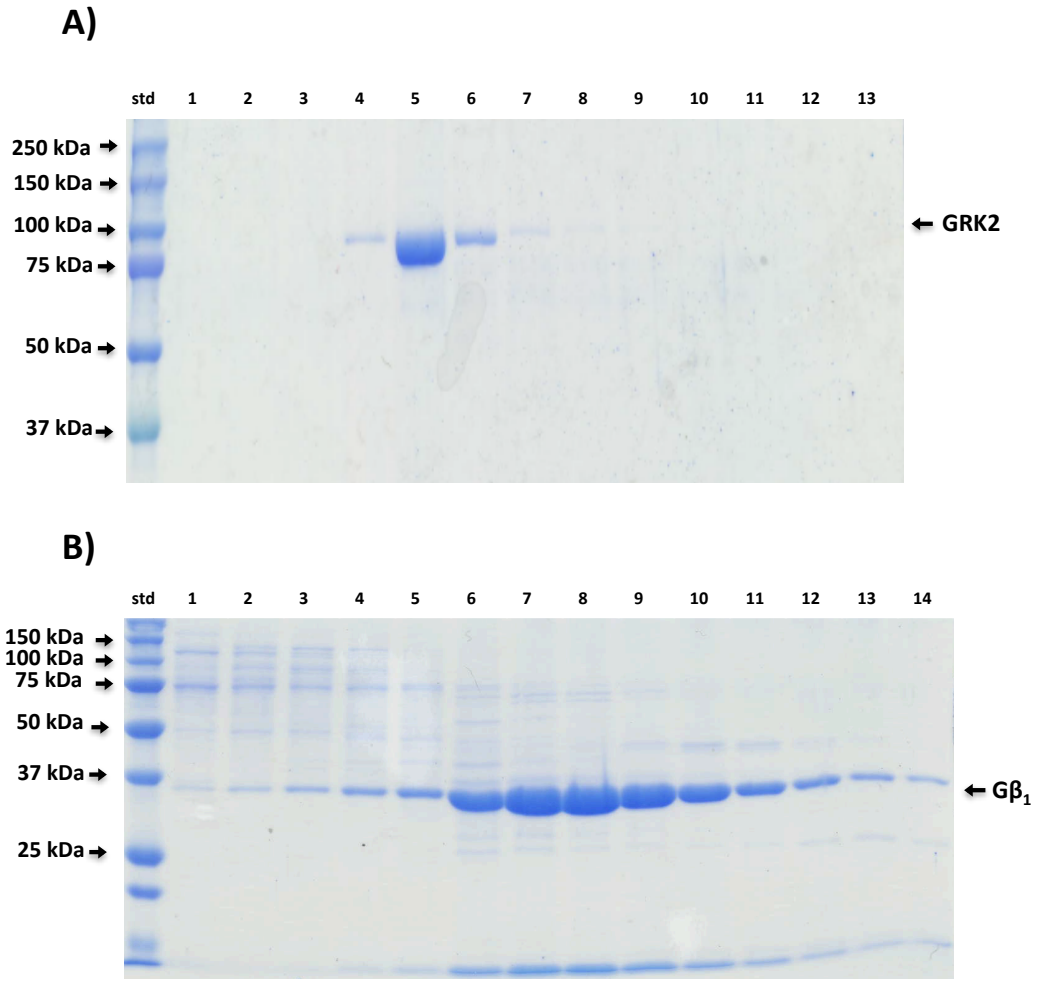

Figure 3.3. Purification of GRK2 and $G\beta_1\gamma_2$ used in SFG and AFTIR spectroscopy experiments. A. Coomassie-stained SDS-PAGE gel of the S200 elution fractions from a representative purification of GRK2. The formula weight of GRK2 is approximately 82 kDa. B. The elution fractions from a representative S200 run of $G\beta_1\gamma_2$ were analyzed as in A. Upon treatment with Laemmli sample buffer the Gβγ dimer dissociates resulting in the band, corresponding to the Gβ subunit, with an apparent molecular weight of 32 kDa.

Expression and purification of soluble $G\beta_1\gamma_2$ for GRK2-Gβγ complex formation

Soluble human $G\beta_1\gamma_2$ containing an N-terminally hexahistidine-tagged β subunit and the C68S mutation was expressed using a dual promoter insect cell expression vector (a gift from Dr. Brian Kobilka) in High Five cells and harvested 48 h post-infection. $G\beta_1\gamma_2$ (C68S) was purified from clarified lysate using nickel-nitrilotriacetic acid affinity and anion exchange chromatography as described previously [64] Fractions containing $G\beta_1\gamma_2$ (C68S) were subsequently

pooled and gel filtered into 20 mM HEPES pH 8.0, 100 mM NaCl, and 1 mM DTT using a S200 column. Purified proteins were concentrated to 10–12 mg/mL as determined by Bradford analysis in a 30 kD cutoff Amicon Ultra-15 centrifugal filter unit, flash frozen in liquid nitrogen, and stored at −80 °C until future use.

Crystal Structure Determination of 14as

For the 14as co-crystal structure, bovine GRK2 and human $G\beta_1\gamma_2$ were added, in a 1:1 molar ratio, to a buffer solution composed of 20 mM HEPES pH 8, 100 mM NaCl, 10 mM CHAPS, 5 mM MgCl2, and 2 mM DTT. This solution was concentrated to approximately 12 mg/mL. A final concentration of 500 μM inhibitor was added to this concentrated solution from a 25 mM stock in 50% DMSO. This solution was then stored on ice for 1 h and filtered through a 0.2 μm Nanosep centrifugal device prior to the assembly of crystal trays. All inhibitor complexes were crystallized at 4 °C by vapor diffusion using hanging drops consisting of 0.8 μL of GRK2-Gβγ–inhibitor complex and 0.8 μL of reservoir solution which contained 100 mM MES pH 6.4–6.7, 200 mM NaCl, and 8–10% PEG 3350. Crystals appeared after 3 days and continued to grow for 1–2 weeks. Crystals were harvested in a cryoprotectant solution containing the contents of the reservoir solution supplemented with 25% ethylene glycol and 500 μM inhibitor and were flash frozen in liquid nitrogen. Diffraction data were collected at the Advanced Photon Source on the LS-CAT beamline 21-ID-D. Data were integrated and scaled using XDS (14as) [95]. Initial phases were calculated using Phaser molecular replacement with ligand-free 3V5W as the search model. Refinement was conducted with phenix.refine, a part of the PHENIX suite, alternating with manual building in Coot. Early in refinement, the dihedral angles from 3V5W were used as restraints. The final model (Fig. 3.4) and structure factors for 14as were validated with

MolProbity[96] (Table 3.1) prior to deposition into the Protein Data Bank under accession code 5UKM.

Table 3.1 Crystal refinement statistics for 5UKM*,[91].

Protein Complex	GRK2-Gβγ·**14as**
X-ray source	APS 21-ID-D
wavelength (Å)	0.9785
D_{min} (Å)	30-3.0 (3.04-3.03)
space group	*C*2
unit cell constants (Å)	*a*=189.0, *b*=74.2, *c*=123.2
(˚)	*β*=115.5
unique reflections	29942 (4657)
R_{sym} (%)	12.9
completeness (%)	98.5
$\langle I \rangle / \langle \sigma_I \rangle$	12.8 (2.0)
redundancy	6.8 (6.8)
refinement resolution (Å)	30.00-3.03 (3.14-3.03)
total reflections used	207836
RMSD bond lengths (Å)	0.012
RMSD bond angles (˚)	1.56
est. coordinate error (Å)	0.404
Ramachandran Plot:	
most favored, allowed, outliers (%)	93.2, 5.3, 1.8
R_{work}	0.1971
R_{free}	0.2516
protein atoms	8192
water molecules	23
inhibitor atoms	33
average *B*-factor (Å^2)	105.0
protein	105.0
inhibitor	123.3
MolProbity score	1.74
MolProbity % C*β* deviations	0
MolProbity % bad backbone bonds	0.01
MolProbity % bad backbone angles	0.01
PDB entry	5UKM

*Entries in parenthesis denote data in the highest resolution shell.

Results and Discussion

The role of lipid composition on the membrane orientation of the GRK2-Gβγ complex

The contributions of the membrane to the function of proteins such GRK2 is not easily accounted for in reconstituted systems. Yet, it seems likely that proper alignment of the kinase domain of GRK2 with respect to its native substrate, activated GPCRs, is important for its function. In order to address this question, we applied the aforementioned combined vibrational spectroscopy method to measure the membrane orientation of both Gβγ and the Gβγ-GRK2 complex on model membranes composed of 1-palmitoyl-2-oleoylphosphatidylcholine and either 1-palmitoyl-2-oleoyl-sn-glycero-3-phospho-(1'-rac-glycerol) or PIP2. Our results suggest that concerted binding of the PH domain to both Gβγ and PIP2 induce a specific orientation in GRK2 that promotes receptor phosphorylation by optimizing the relative position of the receptor-docking site.

The predicted changes in orientation upon binding of PIP2 help explain previous biochemical data supporting a regulatory role for PIP2 in the phosphorylation of active GPCRs and highlight the importance of the PH domain in mediating the function of GRK2. Importantly, neither the use of PIP2 binding-deficient mutants of GRK2 or substitution of PIP2 for a different anionic phospholipid produced such effects providing further support for a specific role of PIP2 in eliciting the observed effects.

Structure-based design of selective and potent inhibitors of GRK2

Because of its prominent role in heart failure, GRK2 has emerged as an attractive target for the development of therapeutics. Our efforts to develop potent and selective GRK2 inhibitors have centered on the structural analysis of known GRK2 inhibitors leading to development of

several promising compounds. As predicted, extension of the fluorophenyl groups of both paroxetine and GSK180736A into the hydrophobic subsite resulted in compounds that exhibit increased potency. Among these novel GRK2 inhibitors, 14as exhibits a nearly 50-fold increase (Table 3.2) in potency relative to its parent compound. Importantly, 14as retained selectivity for GRK2 and exhibits improved efficacy and bioavailability over paroxetine demonstrating the effectiveness of the originally proposed structure guided development of potent and inhibitors of GRK2.

Table 3.2 Kinase inhibitory activity of 14as and its parent scaffold, paroxetine against select AGC kinases[91].

	GRK2 IC50 (μM)	GRK1 IC50 (μM)	GRK5 IC50 (μM)	PKA IC50 (μM)	ROCK*
Paroxetine	1.38±1.00	>100	>100	>100	10%
14as	0.03±0.001	87.3±27.9	7.09±0.73	>100	9%

*Reported as %inhibition at 10μM inhibitor concentration.

Initial SAR indicated that the despite the similarities in binding mode between paroxetine and GSK180736A, the strategy previously employed in the generation of GSK180736A hybrid compounds was incompatible with the paroxetine scaffold. Subsequently, a series of pyridyl methylamides were tested. Of these the 2-pyridine, 14ak exhibited the greatest increase in potency. Further substitution of the amide substituent for 3-pyrazolylmethyl amide resulted in the generation of 14as.

The co-crystal structure of 14as was determined in the space group C2 at a resolution of 3.0 Å. Within the binding pocket the position of the A, B and C rings of 14as nearly matches that

of paroxetine (Fig. 3.4). As with the GSK180736A hybrid series, the carbonyl from the amide forms a hydrogen bond with the backbone nitrogen of Gly201 of the P-loop.

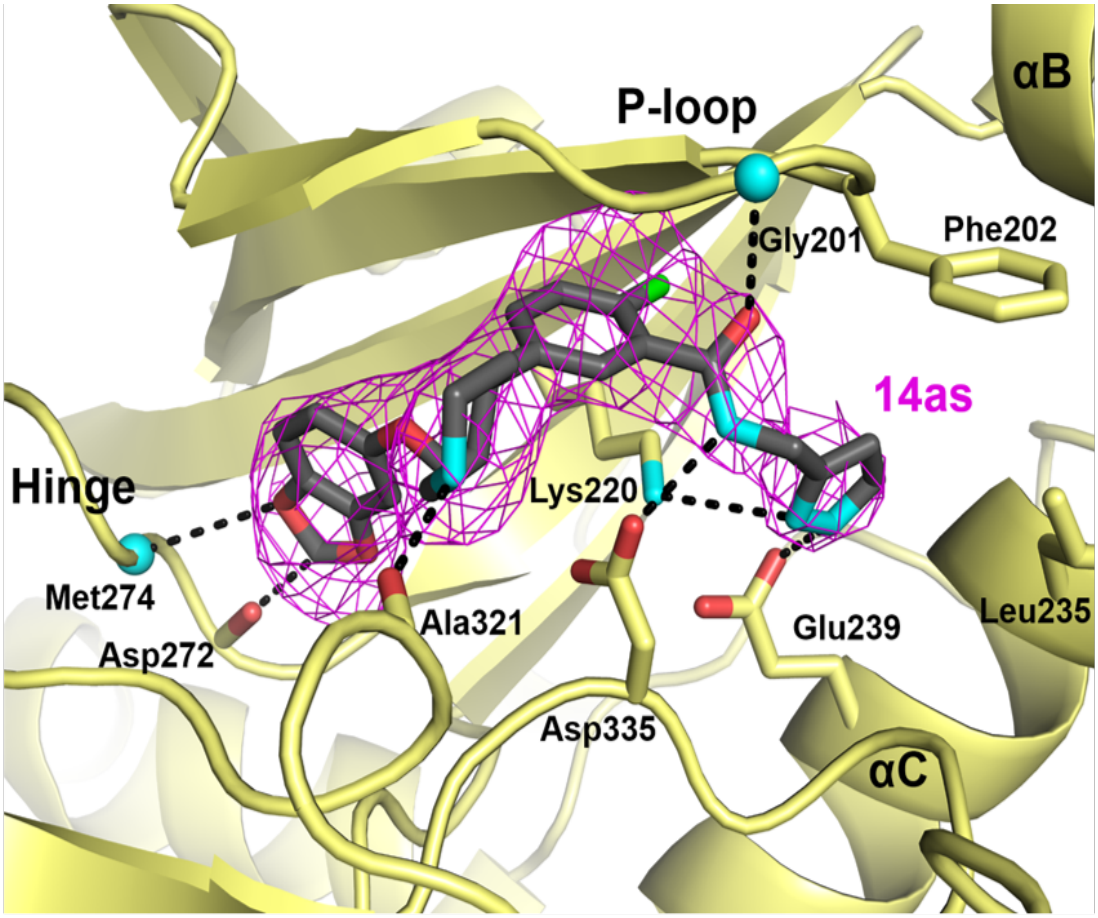

Figure 3.4. Binding mode of 14as in the active site of GRK2. The 3σ $|F_o|-|F_c|$ omit maps of **14as** (magenta wire cage), superimposed on the fully refined 14as-GRK2-Gβγ co-crystal structure, reveals the much like the Takeda compounds described previously[90], 14as engages the hydrophobic subsite . Hydrogen bonding between 14as and select GRK2 residues are represented as black dashed lines.

An additional hydrogen bond is formed between the side chain of Asp335 and the amide nitrogen. Beyond the amide linker, additional hydrogen bonds between the pyrazole nitrogens and residues within the hydrophobic subsite pack the pyrazole moiety in a way that does not require displacement of the αB helix of the small lobe which likely accounts for its increased

potency. My contributions to these projects provided practical experience in x-ray crystallography as well as deeper appreciation for the role of the membrane and its lipid components in modulating the activity of Gβγ effectors.

CHAPTER 4

CONCLUSIONS

The central theme of the thesis presented here is how Gβγ regulates the activities of canonical effectors such as PLCβ and GRK2. Notably, the PH domains of either effector are critical for their interactions with Gβγ and yet, despite their structural similarities, the mode in which this regulatory domain modulates the activity of the intact enzyme diverges. Chapter 2 focused on the role of the PH domain in the Gβγ mediated response of PLCβ isoforms. Although previous studies have shown direct binding of Gβγ to isolated PH domains the structural determinants of the interaction have not been clearly defined. Peptide arrays were used to screen the minimal sequence of PLCβ3 that maintains responsiveness towards Gβγ in an attempt to define the critical residues for binding. The lack of specific binding between the peptides contained within the array and Gβγ hints at the complexity of the binding surface and the potential role of the plasma membrane in possibly enhancing the affinity of the interaction.

We also examined the role of several solvent exposed loops of the PH domain and PH domain-EF hand interface in the activation of PLCβ by Gβγ. Here we found that although the loops connecting β-strands 3 and 4 as well as 5 and 6 of the PH domain and α-helices 1 and 2 of the EF hands do not strongly interact with Gβγ on their own, they are clearly important for activation. Disruption of Gβγ-promoted activity was only apparent by deletion of the

loops whereas substitution with the corresponding sequences from a Gβγ insensitive PLCβ isoform had no effect on the Gβγ mediate response. Importantly, the deletion mutants retained the ability to hydrolyze PIP2 in the absence of Gβγ indicating that the diminished response to Gβγ was not the result of a folding defect. These results provide further support for the importance of the PH domain in the Gβγ mediated response of PLCβ isozymes. In light of the effects of deletion of the solvent exposed loops examined here, diminished Gβγ response without loss of binding, it is tempting to speculate that the PH domain functions as an allosteric conduit of the stimulatory signal triggered by direct contact with Gβγ. The structural consequence of this stimulatory signal is unclear and could just as easily be attributed to a change in membrane orientation of the PLCβ core.

Evidently, determination of the structure of a PLCβ-Gβγ complex has the potential to vastly inform our understanding of the mechanism associated with Gβγ-promoted activation of PLCβ isozymes. Structural characterization of this complex, however, presents unique challenges that must be considered carefully when evaluating potential strategies. First and foremost is the observation that the interaction is relatively weak in the absence of a lipid environment. Previous FRET based estimates of the affinity of PLCβ2 and PLCβ3 towards Gβγ suggests bulk phase dissociation constants in the order of 10-100 μM [97]. The same study estimated that apparent affinity for the lateral association of PLCβ2 and Gβγ on membrane was approximately 10 nM. While this does not imply that conventional vapor diffusion methods would be unfruitful it does highlight the role of the membrane in mediating the interaction.

Intriguingly, several of the recently proposed activation models argue that conformational dynamics of PLCβ isozymes play a central role in its activation by Gβγ [35,37]. This, despite the fact that the available structural data does not support such conformational flexibility, backbone

conformations of all PLCβ structures is nearly identical. These structures, however, were all determined in the absence of lipids. Recently, a study used experimental data gathered from deuterium exchange experiments to guide molecular dynamic simulations that strongly suggest that the membrane acts as an allosteric activator of a different phospholipase, PLA_2 [98]. Notably, structural data of PLA_2 obtained from x-ray crystallography experiments in the absence of lipids or membranes were initially used to argue a lack of conformational flexibility [99]. Whether PLCβ isozymes undergo such conformational changes upon membrane association or effector binding in their native context remains an elusive question.

Chapter 2 also describes the development of an alternative assay for measuring both basal and Gβγ-stimulated activity of PLCβ. In its current state the assay merely serves as a proof of principle and requires more detailed characterization. Several assay parameters, such as substrate, enzyme and Ca^{2+} concentrations and reaction temperature have not yet been fully optimized. Another important assay parameter is the substrate diluent. Previous studies have reported substrate carrier dependent changes in activity of PLCβ2 when either PIP2 or PI are presented in vesicles or micelles of varying composition [75,78]. Notably, the %mol of PE of the lipid vesicles tested here (29%) is different from that of the standard radiometric assay (80%). How such a marked difference in composition might alter the activity of PLCβ in the context of the new assay format is unclear but differences in physical properties of the lipid vesicles have been shown previously to alter the activation of PLCβ2 [100].

Chapter 3 details my contribution to studies aimed at examining the effect of PIP2 on the orientation of the GRK2-Gβγ and the development of potent and selective small molecule inhibitors of GRK2. These studies highlight the functional differences between the PH domains of PLCβ and GRK2. First, unlike the PH domain of PLCβ, which binds non-specifically to

lipids, the PH domain of GRK2 binds to PIP2 and our results argue that the presence of PIP2 in the bilayer alters the orientation of relative position of the kinase domain in a manner facilitates phosphorylation of active GPCRs. Another key difference is the affinity of the GRK2 PH domain for Gβγ subunits, a feature that has been exploited previously to probe Gβγ signaling pathways [101,102].

REFERENCES

1. Kobilka, B. K. G protein coupled receptor structure and activation. *Biochim. Biophys. Acta* **1768,** 794–807 (2007).
2. Overington, J. P., Al-lazikani, B. & Hopkins, A. L. How many drug targets are there ? **5,** 993–996 (2006).
3. Pavlos, N. J. & Friedman, P. A. GPCR Signaling and Trafficking : The Long and Short of It. **28,** 213–226 (2017).
4. Ritter, S. L. & Hall, R. A. Fine-tuning of GPCR activity by receptor-interacting proteins. **10,** 819–830 (2009).
5. Venkatakrishnan, a J. *et al*. Molecular signatures of G-protein-coupled receptors. *Nature* **494,** 185–194 (2013).
6. Hamm, H. E. and A. G. Heterotrimeric G proteins. *Curr. Opin. Cell Biol.* **8,** (1996).
7. Smrcka, a. V. G protein βγ subunits: Central mediators of G protein-coupled receptor signaling. *Cell. Mol. Life Sci.* **65,** 2191–2214 (2008).
8. Dupré, D. J., Robitaille, M., Rebois, R. V. & Hébert, T. E. The role of Gbetagamma subunits in the organization, assembly, and function of GPCR signaling complexes. *Annu. Rev. Pharmacol. Toxicol.* **49,** 31–56 (2009).
9. Khan, S. M. *et al*. The Expanding Roles of G bg Subunits in G Protein – Coupled Receptor Signaling and Drug Action. 545–577 (2013).
10. Clapham, D. E. & Neer, E. J. G PROTEIN βγ SUBUNITS. 167–203 (1997).
11. Clarke, S. Protein Isoprenylation and Methylation at Carboxyl-Terminal Cysteine Residues. *Annu. Rev. Biochem.* **61,** 355–386 (1992).
12. Kalman, V. K., Erdman, R. A., Maltese, W. A. & Robishaw, J. D. Regions outside of the CAAX motif influence the specificity of prenylation of G protein γ subunits. *J. Biol. Chem.* **270,** 14835–14841 (1995).
13. Myung, C. S., Yasuda, H., Liu, W. W., Harden, T. K. & Garrison, J. C. Role of isoprenoid lipids on the heterotrimeric G protein subunit in determining effector activation. *J. Biol. Chem.* **274,** 16595–16603 (1999).
14. Casey, L. M. *et al*. Small molecule disruption of G beta gamma signaling inhibits the progression of heart failure. *Circ Res* **107,** 532–539 (2010).
15. Bonacci, T. M. Differential Targeting of G -Subunit Signaling with Small Molecules. *Science* (2006). doi:10.1126/science.1120378
16. Smrcka, A. V, Lehmann, D. M. & Dessal, A. L. G protein betagamma subunits as targets for small molecule therapeutic development. *Comb. Chem. High Throughput Screen.* **11,** 382–395 (2008).
17. Lehmann, D. M., Seneviratne, A. M. P. B. & Smrcka, A. V. Small molecule disruption of G protein beta gamma subunit signaling inhibits neutrophil chemotaxis and inflammation. *Mol. Pharmacol.* **73,** 410–8 (2008).
18. Rhee, S. G. Regulation of Phosphoinositide-specific Phospholipase C. *Annu Rev Biochem*

70, 281–312 (2001).
19. McLaughlin, S., Wang, J., Gambhir, A. & Murray, D. PIP $_2$ and Proteins: Interactions, Organization, and Information Flow. *Annu. Rev. Biophys. Biomol. Struct.* **31,** 151–175 (2002).
20. Kadamur, G. & Ross, E. M. Mammalian phospholipase C. *Annu Rev Physiol* **75,** 127–154 (2013).
21. Snyder, J. T., Jezyk, M. R., Gershburg, S., Harden, T. K. & Sondek, J. Regulation of PLC beta isoforms by rac. *Methods Enzymol. Vol 406, Regul. Eff. Small Gtpases Rho Fam.* **406,** 272–280 (2006).
22. Wu, D., Katz, A. & Simon, M. I. Activation of phospholipase C beta 2 by the alpha and beta gamma subunits of trimeric GTP-binding protein. *Proc. Natl. Acad. Sci. U. S. A.* **90,** 5297–5301 (1993).
23. Zhou, Y., Sondek, J. & Harden, T. K. Activation of human phospholipase C-eta2 by Gbetagamma. *Biochemistry* **47,** 4410–4417 (2008).
24. Lyon, A. M. & Tesmer, J. J. G. Structural insights into phospholipase C-β function. *Mol. Pharmacol.* **84,** 488–500 (2013).
25. Jezyk, M. R. *et al.* Crystal structure of Rac1 bound to its effector phospholipase C-beta2. *Nat. Struct. Mol. Biol.* **13,** 1135–1140 (2006).
26. Lyon, A. M., Begley, J. a, Manett, T. D. & Tesmer, J. J. G. Molecular mechanisms of phospholipase C β3 autoinhibition. *Structure* **22,** 1844–54 (2014).
27. Charpentier, T. H. *et al.* Membrane-induced Allosteric Control of Phospholipase C-β Isozymes. *J. Biol. Chem.* **289,** 29545–29557 (2014).
28. Lyon, A. M. *et al.* An autoinhibitory helix in the C-terminal region of phospholipase C-β mediates Gα(q) activation. *Nat. Struct. Mol. Biol.* **18,** 999–1005 (2011).
29. Lyon, A. M., Dutta, S., Boguth, C. a, Skiniotis, G. & Tesmer, J. J. G. Full-length Gα(q)-phospholipase C-β3 structure reveals interfaces of the C-terminal coiled-coil domain. *Nat. Struct. Mol. Biol.* **20,** 355–62 (2013).
30. Kuang, Y., Wu, Y., Smrcka, A., Jiang, H. & Wu, D. Identification of a phospholipase C beta2 region that interacts with Gbeta-gamma. *Proc. Natl. Acad. Sci. U. S. A.* **93,** 2964–8 (1996).
31. Sankaran, B., Osterhout, J., Wu, D. & Smrcka, a V. Identification of a structural element in phospholipase C beta2 that interacts with G protein betagamma subunits. *J. Biol. Chem.* **273,** 7148–7154 (1998).
32. Lehmann, D. M., Yuan, C. & Smrcka, A. V. in *Methods in Enzymology* **434,** 29–48 (2007).
33. Mahadevan, D. *et al.* Structural studies on the PH domains of Db1, Sos1, IRS-1, and beta ARK1 and their differential binding to G beta gamma subunits. *Biochemistry* **34,** 9111–9117 (1995).
34. Wang, T., Pentyala, S., Rebecchi, M. J. & Scarlata, S. Differential Association of the Pleckstrin Homology Domains of Phospholipases C- 1 , C- 2 , and C-δ 1 with Lipid Bilayers and the γ Subunits of Heterotrimeric G. 1517–1524 (1999).
35. Kadamur, G. & Ross, E. M. Intrinsic Pleckstrin Homology (PH) Domain Motion in Phospholipase C-β Exposes a Gβγ Protein Binding Site. *J. Biol. Chem.* **291,** 11394–11406 (2016).
36. Wang, T., Dowal, L., El-Maghrabi, M. R., Rebecchi, M. & Scarlata, S. The pleckstrin homology domain of phospholipase C-beta(2) links the binding of gbetagamma to

activation of the catalytic core. *J. Biol. Chem.* **275,** 7466–7469 (2000).
37. Han, D. S., Golebiewska, U., Stolzenberg, S., Scarlata, S. F. & Weinstein, H. A Dynamic Model of Membrane-Bound Phospholipase C{beta}2 Activation by G{beta}{gamma} Subunits. *Mol. Pharmacol.* **80,** 434–445 (2011).
38. Li, J. *et al.* Agonist-induced formation of opioid receptor-G protein-coupled receptor kinase (GRK)-Gβγ complex on membrane is required for GRK2 function in vivo. *J. Biol. Chem.* **278,** 30219–30226 (2003).
39. Pitcher, J. A. *et al.* Role of beta gamma subunits of G proteins in targeting the beta-adrenergic receptor kinase to membrane-bound receptors. *Science* **257,** 1264–7 (1992).
40. Evron, T., Daigle, T. L. & Caron, M. G. GRK2: Multiple roles beyond G protein-coupled receptor desensitization. *Trends Pharmacol. Sci.* **33,** 154–164 (2012).
41. Lymperopoulos, A. GRK2 and β-arrestins in cardiovascular disease: Something old, something new. *Am. J. Cardiovasc. Dis.* **1,** 126–37 (2011).
42. Vroon, A., Heijnen, C. J. & Kavelaars, A. GRKs and arrestins: regulators of migration and inflammation. *J. Leukoc. Biol.* **80,** 1214–1221 (2006).
43. Penela, P., Ribas, C., Aymerich, I. & Mayor, F. New roles of G protein-coupled receptor kinase 2 (GRK2) in cell migration. *Cell Adh. Migr.* **3,** 19–23 (2009).
44. Vinge, L. E. *et al.* Substrate specificities of g protein-coupled receptor kinase-2 and -3 at cardiac myocyte receptors provide basis for distinct roles in regulation of myocardial function. *Mol. Pharmacol.* **72,** 582–91 (2007).
45. Rao, J. S., Rapoport, S. I. & Kim, H.-W. Decreased GRK3 but not GRK2 expression in frontal cortex from bipolar disorder patients. *Int. J. Neuropsychopharmacol.* **12,** 851–60 (2009).
46. Pitcher, J. A., Freedman, N. J. & Lefkowitz, R. J. G protein-coupled receptor kinases. *Annu. Rev. Biochem.* **67,** 653–692 (1998).
47. Homan, K. T. & Tesmer, J. J. G. Molecular Basis for Small Molecule Inhibition of G Protein-Coupled Receptor Kinases. *ACS Chem. Biol.* **10,** 246–256 (2015).
48. Arencibia, J. M., Pastor-Flores, D., Bauer, A. F., Schulze, J. O. & Biondi, R. M. AGC protein kinases: From structural mechanism of regulation to allosteric drug development for the treatment of human diseases. *BBA - Proteins Proteomics* **1834,** 1302–1321 (2013).
49. Kannan, N., Haste, N., Taylor, S. S. & Neuwald, A. F. The hallmark of AGC kinase functional divergence is its C-terminal tail, a cis-acting regulatory module. *Proc. Natl. Acad. Sci. U. S. A.* **104,** 1272–1277 (2008).
50. Guccione, M. *et al.* G-protein-coupled receptor kinase 2 (GRK2) inhibitors: Current trends and future perspectives. *Journal of Medicinal Chemistry* **59,** 9277–9294 (2016).
51. Waldschmidt, H. V. *et al.* Structure-Based Design, Synthesis, and Biological Evaluation of Highly Selective and Potent G Protein-Coupled Receptor Kinase 2 Inhibitors. *J. Med. Chem.* **59,** 3793–3807 (2016).
52. Komolov, K. E., Bhardwaj, A. & Benovic, J. L. Atomic structure of GRK5 reveals distinct structural features novel for G protein-coupled receptor kinases. *J. Biol. Chem.* **290,** 20629–20647 (2015).
53. Homan, K. T. *et al.* Crystal structure of G protein-coupled receptor kinase 5 in complex with a rationally designed inhibitor. *J. Biol. Chem.* **290,** 20649–20659 (2015).
54. Lodowski, D. T. *et al.* The role of G beta gamma and domain interfaces in the activation of G protein-coupled receptor kinase 2. *Biochemistry* **44,** 6958–70 (2005).
55. Boughton *et al.* Heterotrimeric G protein {beta}1{gamma}2 subunits change orientation

upon complex formation with G protein-coupled receptor kinase 2 (GRK2) on a model membrane. *Proc. Natl. Acad. Sci. U. S. A.* **108,** E667-73 (2011).
56. Rebecchi, M. J. & Scarlata, S. Pleckstrin homology domains: a common fold with diverse functions. *Annu. Rev. Biophys. Biomol. Struct.* **27,** 503–528 (1998).
57. Rebecchi, M. J. & Pentyala, S. N. Structure , Function , and Control of Phosphoinositide-Specific Phospholipase C. **80,** 1291–1336 (2000).
58. Drin, G. & Scarlata, S. Stimulation of phospholipase Cβ by membrane interactions, interdomain movement, and G protein binding — How many ways can you activate an enzyme? *Cell. Signal.* **19,** 1383–1392 (2007).
59. Scheffzek, K. & Welti, S. Pleckstrin homology (PH) like domains - Versatile modules in protein-protein interaction platforms. *FEBS Lett.* **586,** 2662–2673 (2012).
60. Blomberg, N., Baraldi, E., Nilges, M. & Saraste, M. The PH superfold: A structural scaffold for multiple functions. *Trends in Biochemical Sciences* **24,** 441–445 (1999).
61. Qi, D. & Scholthof, K. B. G. A one-step PCR-based method for rapid and efficient site-directed fragment deletion, insertion, and substitution mutagenesis. *J. Virol. Methods* (2008). doi:10.1016/j.jviromet.2008.01.002
62. Longo, P. a., Kavran, J. M., Kim, M. S. & Leahy, D. J. *Transient mammalian cell transfection with polyethylenimine (PEI). Methods in Enzymology* **529,** (Elsevier Inc., 2013).
63. Tom, R., Bisson, L. & Durocher, Y. Transfection of HEK293-EBNA1 cells in suspension with linear PEI for production of recombinant proteins. *Cold Spring Harb. Protoc.* **3,** (2008).
64. Kozasa, T. Purification of G Protein Subunits from Sf9 Insect Cells Using Hexahistidine-Tagged α and βγ Subunits. *G Protein Signal.* **237,** 21–38 (2004).
65. Ghosh, M. & Smrcka, A. V. Assay for G protein-dependent activation of phospholipase Cb using purified protein components. *Methods Mol Biol* **237,** 67–75 (2004).
66. Yim, Y. Y., Betke, K. & Hamm, H. Protein-Protein Interactions. **8,** 307–320 (2012).
67. Scott, J. K. *et al.* Evidence that a protein ± protein interaction ` hot spot ' on heterotrimeric G protein bg subunits is used for recognition of a subclass of effectors. **20,** 767–776 (2001).
68. Weng, G. *et al.* Gβ subunit interacts with a peptide encoding region 956-982 of adenylyl cyclase 2. Cross-linking of the peptide to free Gβγ but not the heterotrimer. *J. Biol. Chem.* **271,** 26445–26448 (1996).
69. De Waard, M., Hering, J., Weiss, N. & Feltz, A. How do G proteins directly control neuronal Ca2+ channel function? *Trends in Pharmacological Sciences* **26,** 427–436 (2005).
70. Koch, W. J., Inglese, J., Stone, W. C. & Lefkowitz, R. J. The binding site for the beta gamma subunits of heterotrimeric G proteins on the beta-adrenergic receptor kinase. *J. Biol. Chem.* **268,** 8256–8260 (1993).
71. Katz, C. *et al.* Studying protein-protein interactions using peptide arrays. *Chem. Soc. Rev.* **40,** 2131–2145 (2011).
72. Barr, A. J., Ali, H., Haribabu, B., Snyderman, R. & Smrcka, A. V. Identification of a region at the N-terminus of phospholipase C-beta 3 that interacts with G protein beta gamma subunits. *Biochemistry* **39,** 1800–1806 (2000).
73. Hicks, S. N. *et al.* General and Versatile Autoinhibition of PLC Isozymes. *Mol. Cell* (2008). doi:10.1016/j.molcel.2008.06.018

74. Waldo, G. L. *et al*. Kinetic scaffolding mediated by a phospholipase C-beta and Gq signaling complex. *Science* **330,** 974–980 (2010).
75. Drin, G., Douguet, D. & Scarlata, S. The Pleckstrin Homology Domain of Phospholipase Cβ Transmits Enzymatic Activation through Modulation of the Membrane–Domain Orientation †. *Biochemistry* **45,** 5712–5724 (2006).
76. Rhee, S., Suh, P., Ryu, S. & Lee, S. Studies of inositol phospholipid-specific phospholipase C. *Science (80-.).* **244,** 546–550 (1989).
77. Hofmann, S. L. & Majerus, P. W. Modulation of phosphatidylinositol-specific phospholipase C activity by phospholipid interactions, diglycerides, and calcium ions. *J. Biol. Chem.* **257,** 14359–14364 (1982).
78. Feng, J., Roberts, M. F., Drin, G. & Scarlata, S. Dissection of the steps of phospholipase C beta 2 activity that are enhanced by G beta gamma subunits. *Biochemistry* **44,** 2577–84 (2005).
79. Jenco, J. M., Becker, K. P. & Morris, a J. Membrane-binding properties of phospholipase C-beta1 and phospholipaseC-beta2: role of the C-terminus and effects of polyphosphoinositides, G-proteins and Ca2+. *Biochem. J.* **327 (Pt 2,** 431–437 (1997).
80. Bonacci, T. M., Ghosh, M., Malik, S. & Smrcka, A. V. Regulatory Interactions between the Amino Terminus of G-protein βγ Subunits and the Catalytic Domain of Phospholipase Cβ2. *J. Biol. Chem.* **280,** 10174–10181 (2005).
81. Illenberger, D., Walliser, C., Nürnberg, B., Lorente, M. D. & Gierschik, P. Specificity and structural requirements of phospholipase C-β stimulation by Rho GTPases versus G protein βγ dimers. *J. Biol. Chem.* (2003). doi:10.1074/jbc.M208282200
82. Gurevich, E. V., Tesmer, J. J. G., Mushegian, A. & Gurevich, V. V. G protein-coupled receptor kinases: More than just kinases and not only for GPCRs. *Pharmacol. Ther.* **133,** 40–69 (2012).
83. Pitcher, J. A. *et al*. Phosphatidylinositol 4,5-bisphosphate (PIP2)-enhanced G protein-coupled receptor kinase (GRK) activity. Location, structure, and regulation of the PIP2 binding site distinguishes the GRK families. *J. Biol. Chem.* **271,** 24907–24913 (1996).
84. DebBurman, S. K., Ptasienski, J., Benovic, J. L. & Hosey, M. M. G protein-coupled receptor kinase GRK2 is a phospholipid-dependent enzyme that can be conditionally activated by G protein βγ subunits. *J. Biol. Chem.* **271,** 22552–22562 (1996).
85. Yang, P., Glukhova, A., Tesmer, J. J. G. & Chen, Z. Membrane orientation and binding determinants of G protein-coupled receptor kinase 5 as assessed by combined vibrational spectroscopic studies. *PLoS One* **8,** (2013).
86. Chen, X., Boughton, A. P., Tesmer, J. J. G. & Chen, Z. In Situ Investigation of Heterotrimeric G Protein βγ Subunit Binding and Orientation on Membrane Bilayers. *J. Am. Chem. Soc.* **129,** 12658–12659 (2007).
87. Yang, P., Boughton, A., Homan, K. T., Tesmer, J. J. G. & Chen, Z. Membrane orientation of Gαiβ1γ 2 and Gβ1γ2 determined via combined vibrational spectroscopic studies. *J. Am. Chem. Soc.* **135,** 5044–5051 (2013).
88. Yang, P. *et al*. Effect of Lipid Composition on the Membrane Orientation of the G Protein-Coupled Receptor Kinase 2-Gβ1γ2 Complex. *Biochemistry* **55,** 2841–2848 (2016).
89. Rockman, H. a, Koch, W. J. & Lefkowitz, R. J. Seven-transmembrane-spanning receptors and heart function. *Nature* **415,** 206–212 (2002).
90. Thal, D. M., Yeow, R. Y., Schoenau, C., Huber, J. & Tesmer, J. J. G. Molecular

mechanism of selectivity among G protein-coupled receptor kinase 2 inhibitors. *Mol. Pharmacol.* **80,** 294–303 (2011).
91. Waldschmidt, H. V. *et al.* Structure-Based Design of Highly Selective and Potent G Protein-Coupled Receptor Kinase 2 Inhibitors Based on Paroxetine. *J. Med. Chem.* **60,** 3052–3069 (2017).
92. Thal, D. M. *et al.* Paroxetine is a direct inhibitor of G protein-coupled receptor kinase 2 and increases myocardial contractility. *ACS Chem. Biol.* **7,** 1830–1839 (2012).
93. Homan, K. T. *et al.* Identification and Structure–Function Analysis of Subfamily Selective G Protein-Coupled Receptor Kinase Inhibitors. *ACS Chem. Biol.* **10,** 310–319 (2014).
94. Lodowski, D. T. *et al.* Purification, crystallization and preliminary X-ray diffraction studies of a complex between G protein-coupled receptor kinase 2 and Gbeta1gamma2. *Acta Crystallogr. D. Biol. Crystallogr.* **59,** 936–939 (2003).
95. Kabsch, W. XDS. *Acta Crystallogr. Sect. D Biol. Crystallogr.* **66,** 125–132 (2010).
96. Chen, V. B. *et al.* MolProbity: All-atom structure validation for macromolecular crystallography. *Acta Crystallogr. Sect. D Biol. Crystallogr.* **66,** 12–21 (2010).
97. Effectors, T. P. C.-, Runnels, L. W. & Scarlata, S. F. Determination of the Affinities between Heterotrimeric G Protein Subunits and. 1488–1496 (1999).
98. Mouchlis, V. D., Bucher, D., McCammon, J. A. & Dennis, E. a. Membranes serve as allosteric activators of phospholipase A2, enabling it to extract, bind, and hydrolyze phospholipid substrates. *Proc. Natl. Acad. Sci.* **112,** E516–E525 (2015).
99. Tatulian, S. a. Toward understanding interfacial activation of secretory phospholipase A2 (PLA2): membrane surface properties and membrane-induced structural changes in the enzyme contribute synergistically to PLA2 activation. *Biophys. J.* **80,** 789–800 (2001).
100. Arduin, A., Gaffney, P. R. & Ces, O. Regulation of PLCbeta2 by the electrostatic and mechanical properties of lipid bilayers. *Sci Rep* **5,** 12628 (2015).
101. Inglese, J. *et al.* Functionally active targeting domain of the beta-adrenergic receptor kinase: an inhibitor of G beta gamma-mediated stimulation of type II adenylyl cyclase. *Proc. Natl. Acad. Sci. U. S. A.* **91,** 3637–3641 (1994).
102. Huynh, T. T. T. *et al.* Adenoviral-mediated inhibition of Gβγ signaling limits the hyperplastic response in experimental vein grafts. *Surgery* **124,** 177–186 (1998).
103. Waldschmidt, H. V *et al.* Structure-Based Design, Synthesis, and Biological Evaluation of Highly Selective and Potent G Protein-Coupled Receptor Kinase 2 Inhibitors. *J. Med. Chem.* **59,** 3793–3807 (2016).